

# A Lagrange multiplier method for a Stokes-Biot fluid-poroelastic structure interaction model

Ilna Ambartsumyan\* Eldar Khattatov\* Ivan Yotov\* Paolo Zunino<sup>†‡</sup>

August 13, 2018

## Abstract

We study a finite element computational model for solving the coupled problem arising in the interaction between a free fluid and a fluid in a poroelastic medium. The free fluid is governed by the Stokes equations, while the flow in the poroelastic medium is modeled using the Biot poroelasticity system. Equilibrium and kinematic conditions are imposed on the interface. A mixed Darcy formulation is employed, resulting in continuity of flux condition of essential type. A Lagrange multiplier method is employed to impose weakly this condition. A stability and error analysis is performed for the semi-discrete continuous-in-time and the fully discrete formulations. A series of numerical experiments is presented to confirm the theoretical convergence rates and to study the applicability of the method to modeling physical phenomena and the sensitivity of the model with respect to its parameters.

## 1 Introduction

In this paper we study the interaction of a free incompressible viscous Newtonian fluid with a fluid within a poroelastic medium. This is a challenging multiphysics problem with applications to predicting and controlling processes arising in groundwater flow in fractured aquifers, oil and gas extraction, arterial flows, and industrial filters. In these applications, it is important to model properly the interaction between the free fluid with the fluid within the porous medium, and to take into account the effect of the deformation of the medium. For example, geomechanical effects play an important role in hydraulic fracturing, as well as in modeling phenomena such as subsidence and compaction.

We adopt the Stokes equations to model the free fluid and the Biot system [6] for the fluid in the poroelastic media. In the latter, the volumetric deformation of the elastic porous matrix is complemented with the Darcy equation that describes the average velocity of the fluid in the pores. The model features two different kinds of coupling across the interface: Stokes-Darcy coupling [17, 26, 32, 40, 45, 51, 52] and fluid-structure interaction (FSI) [4, 16, 41, 42, 53].

The well-posedness of the mathematical model based on the Stokes-Biot system for the coupling between a fluid and a poroelastic structure is studied in [48]. A numerical study of the problem, using the Navier-Stokes equations for the fluid, is presented in [4], utilizing a variational multiscale approach to stabilize the finite element spaces. The problem is solved using both a monolithic and a

---

\*Department of Mathematics, University of Pittsburgh, Pittsburgh, PA 15260, USA; [ila6@pitt.edu](mailto:ila6@pitt.edu), [elk58@pitt.edu](mailto:elk58@pitt.edu), [yotov@math.pitt.edu](mailto:yotov@math.pitt.edu); partially supported by DOE grant DE-FG02-04ER25618 and NSF grant DMS 1418947.

<sup>†</sup>Department of Mechanical Engineering & Materials Science, Pittsburgh, PA 15261, USA; [paz13@pitt.edu](mailto:paz13@pitt.edu); partially supported by DOE grant DE-FG02-04ER25618.

<sup>‡</sup>MOX, Department of Mathematics, Politecnico di Milano, Italy.

partitioned approach, with the latter requiring subiterations between the two problems. The reader is also referred to [10], where a non-iterative operator-splitting method for a coupled Navier-Stokes-Biot model is developed.

An alternative partitioned approach for the coupled Stokes-Biot problem based on the Nitsche's method is developed in [9]. The resulting method is loosely coupled and non-iterative with conditional stability. Unlike the method in [10], which is suitable for the pressure formulation of Darcy flow, the Nitsche's method can handle the mixed Darcy formulation. It does, however, suffer from a reduced convergence, due to the splitting across the interface. This is typical for Nitsche's splittings, see e.g. [12] for modeling of FSI. Possible approaches to alleviate this problem include iterative correction [13] and the use of the split method as a preconditioner for the monolithic scheme [9].

In applications to flow in fractured poroelastic media, an alternative modeling approach is based on a reduced-dimension fracture model. We mention recent work using the Reynolds lubrication equation [24,28,33,38] as well as an averaged Brinkman equation [11]. Earlier works that do not account for elastic deformation of the media include averaged Darcy models [15, 20, 22, 36, 39], Forchheimer models [21], and Brinkman models [34].

In this work we focus on the monolithic scheme for the full-dimensional Stokes-Biot problem with the approximation of the continuity of normal velocity condition through the use of a Lagrange multiplier. We consider the mixed formulation for Darcy flow in the Biot system, which provides a locally mass conservative flow approximation and an accurate Darcy velocity. However, this formulation results in the continuity of normal velocity condition being of essential type, which requires weak enforcement through either a penalty or a Lagrange multiplier formulation. Here we study the latter, as an alternative to the previously developed Nitsche formulation [9]. The advantage of the Lagrange multiplier method is that it doesn't involve a penalty parameter and it can enforce the the continuity of normal velocity with machine precision accuracy on matching grids [1]. The method is also convergent on non-matching grids. After deriving a finite element based numerical approximation scheme for the Stokes-Biot problem, we provide a detailed theoretical analysis of stability and error estimates. A critical component of the analysis is the construction of a finite element interpolant in the space of velocities with weakly continuous normal components. This interpolant is shown to have optimal approximation properties, even for grids that do not match across the interface. The numerical tests confirm the theoretical convergence rates and illustrate that the method is applicable for simulating real world phenomena with a wide range of realistic physical parameters.

An additional advantage of the Lagrange multiplier formulation is that it is suitable for efficient parallel domain decomposition algorithms for the solution of the coupled problem, via its reduction to an interface problem, see, e.g. [51] for the Stokes-Darcy problem. It can also lead to multiscale approximations through the use of a coarse-scale Lagrange multiplier or mortar space [2,25,27]. However, this topic is beyond the scope of the paper and it will be investigated in the future.

The remainder of the manuscript is organized as follows. In Section 2 we present the mathematical model. Section 3 is devoted to the semi-discrete continuous-in-time numerical scheme and the uniqueness and existence of its solution, followed by its stability analysis in Section 4. A detailed error analysis is presented in Section 5, which gives insight on the expected convergence rates with different choice of finite element spaces. Section 6 and the Appendix present the analysis for the fully discrete scheme. Extensive numerical experiments are discussed in Section 7, while Section 8 sums up our findings.

## 2 Stokes-Biot model problem

We consider a multiphysics model problem for free fluid's interaction with a flow in a deformable porous media, where the simulation domain  $\Omega \subset \mathbf{R}^d$ ,  $d = 2, 3$ , is a union of non-overlapping regions  $\Omega_f$  and  $\Omega_p$ . Here  $\Omega_f$  is a free fluid region with flow governed by the Stokes equations and  $\Omega_p$  is a poroelastic material governed by the Biot system. For simplicity of notation, we assume that each region is connected. The extension to non-connected regions is straightforward. Let  $\Gamma_{fp} = \partial\Omega_f \cap \partial\Omega_p$ . Let  $(\mathbf{u}_\star, p_\star)$  be the velocity-pressure pair in  $\Omega_\star$ ,  $\star = f, p$ , and let  $\boldsymbol{\eta}_p$  be the displacement in  $\Omega_p$ . Let  $\mu > 0$  be the fluid viscosity, let  $\mathbf{f}_\star$  be the body force terms, and let  $q_\star$  be external source or sink terms. Let  $\mathbf{D}(\mathbf{u}_f)$  and  $\boldsymbol{\sigma}_f(\mathbf{u}_f, p_f)$  denote, respectively, the deformation rate tensor and the stress tensor:

$$\mathbf{D}(\mathbf{u}_f) = \frac{1}{2}(\nabla\mathbf{u}_f + \nabla\mathbf{u}_f^T), \quad \boldsymbol{\sigma}_f(\mathbf{u}_f, p_f) = -p_f\mathbf{I} + 2\mu\mathbf{D}(\mathbf{u}_f).$$

In the free fluid region  $\Omega_f$ ,  $(\mathbf{u}_f, p_f)$  satisfy the Stokes equations

$$-\nabla \cdot \boldsymbol{\sigma}_f(\mathbf{u}_f, p_f) = \mathbf{f}_f \quad \text{in } \Omega_f \times (0, T] \quad (2.1)$$

$$\nabla \cdot \mathbf{u}_f = q_f \quad \text{in } \Omega_f \times (0, T], \quad (2.2)$$

where  $T > 0$  is the final time. Let  $\boldsymbol{\sigma}_e(\boldsymbol{\eta}_p)$  and  $\boldsymbol{\sigma}_p(\boldsymbol{\eta}_p, p_p)$  be the elastic and poroelastic stress tensors, respectively:

$$\boldsymbol{\sigma}_e(\boldsymbol{\eta}_p) = \lambda_p(\nabla \cdot \boldsymbol{\eta}_p)\mathbf{I} + 2\mu_p\mathbf{D}(\boldsymbol{\eta}_p), \quad \boldsymbol{\sigma}_p(\boldsymbol{\eta}_p, p_p) = \boldsymbol{\sigma}_e(\boldsymbol{\eta}_p) - \alpha p_p\mathbf{I}, \quad (2.3)$$

where  $0 < \lambda_{min} \leq \lambda_p(\mathbf{x}) \leq \lambda_{max}$  and  $0 < \mu_{min} \leq \mu_p(\mathbf{x}) \leq \mu_{max}$  are the Lamé parameters and  $0 \leq \alpha \leq 1$  is the Biot-Willis constant. The poroelasticity region  $\Omega_p$  is governed by the quasi-static Biot system [6]

$$-\nabla \cdot \boldsymbol{\sigma}_p(\boldsymbol{\eta}_p, p_p) = \mathbf{f}_p, \quad \mu K^{-1}\mathbf{u}_p + \nabla p_p = 0, \quad \text{in } \Omega_p \times (0, T], \quad (2.4)$$

$$\frac{\partial}{\partial t} (s_0 p_p + \alpha \nabla \cdot \boldsymbol{\eta}_p) + \nabla \cdot \mathbf{u}_p = q_p \quad \text{in } \Omega_p \times (0, T], \quad (2.5)$$

where  $s_0 \geq 0$  is a storage coefficient and  $K$  the symmetric and uniformly positive definite rock permeability tensor, satisfying, for some constants  $0 < k_{min} \leq k_{max}$ ,

$$\forall \boldsymbol{\xi} \in \mathbf{R}^d, \quad k_{min}\boldsymbol{\xi}^T \boldsymbol{\xi} \leq \boldsymbol{\xi}^T K(\mathbf{x})\boldsymbol{\xi} \leq k_{max}\boldsymbol{\xi}^T \boldsymbol{\xi}, \quad \forall \mathbf{x} \in \Omega_p.$$

Following [4, 48], the *interface conditions* on the fluid-poroelasticity interface  $\Gamma_{fp}$  are *mass conservation*, *balance of stresses*, and the Beavers-Joseph-Saffman (BJS) condition [5, 46] modeling *slip with friction*:

$$\mathbf{u}_f \cdot \mathbf{n}_f + \left( \frac{\partial \boldsymbol{\eta}_p}{\partial t} + \mathbf{u}_p \right) \cdot \mathbf{n}_p = 0 \quad \text{on } \Gamma_{fp} \times (0, T], \quad (2.6)$$

$$-(\boldsymbol{\sigma}_f \mathbf{n}_f) \cdot \mathbf{n}_f = p_p, \quad \boldsymbol{\sigma}_f \mathbf{n}_f + \boldsymbol{\sigma}_p \mathbf{n}_p = 0 \quad \text{on } \Gamma_{fp} \times (0, T], \quad (2.7)$$

$$-(\boldsymbol{\sigma}_f \mathbf{n}_f) \cdot \boldsymbol{\tau}_{f,j} = \mu \alpha_{BJS} \sqrt{K_j^{-1}} \left( \mathbf{u}_f - \frac{\partial \boldsymbol{\eta}_p}{\partial t} \right) \cdot \boldsymbol{\tau}_{f,j} \quad \text{on } \Gamma_{fp} \times (0, T], \quad (2.8)$$

where  $\mathbf{n}_f$  and  $\mathbf{n}_p$  are the outward unit normal vectors to  $\partial\Omega_f$ , and  $\partial\Omega_p$ , respectively,  $\boldsymbol{\tau}_{f,j}$ ,  $1 \leq j \leq d-1$ , is an orthogonal system of unit tangent vectors on  $\Gamma_{fp}$ ,  $K_j = (K \boldsymbol{\tau}_{f,j}) \cdot \boldsymbol{\tau}_{f,j}$ , and  $\alpha_{BJS} \geq 0$  is an experimentally determined friction coefficient. We note that the continuity of flux constrains the normal velocity of the solid skeleton, while the BJS condition accounts for its tangential velocity.

The above system of equations needs to be complemented by a set of boundary and initial conditions. Let  $\Gamma_f = \partial\Omega_f \cap \partial\Omega$  and  $\Gamma_p = \partial\Omega_p \cap \partial\Omega$ . Let  $\Gamma_p = \Gamma_p^D \cup \Gamma_p^N$ . We assume for simplicity homogeneous boundary conditions:

$$\mathbf{u}_f = 0 \text{ on } \Gamma_f \times (0, T], \quad \boldsymbol{\eta}_p = 0 \text{ on } \Gamma_p \times (0, T], \quad p_p = 0 \text{ on } \Gamma_p^D \times (0, T], \quad \mathbf{u}_p \cdot \mathbf{n}_p = 0 \text{ on } \Gamma_p^N \times (0, T].$$

To avoid the issue with restricting the mean value of the pressure, we assume that  $|\Gamma_p^D| > 0$ . We also assume that  $\Gamma_p^D$  is not adjacent to the interface  $\Gamma_{fp}$ , i.e.,  $\text{dist}(\Gamma_p^D, \Gamma_{fp}) \geq s > 0$ . Non-homogeneous displacement and velocity conditions can be handled in a standard way by adding suitable extensions of the boundary data. The pressure boundary condition is natural in the mixed Darcy formulation, so non-homogeneous pressure data would lead to an additional boundary term. We further set the initial conditions

$$p_p(\mathbf{x}, 0) = p_{p,0}(\mathbf{x}), \quad \boldsymbol{\eta}_p(\mathbf{x}, 0) = \boldsymbol{\eta}_{p,0}(\mathbf{x}) \text{ in } \Omega_p.$$

The solvability of the Stokes-Biot system (2.1)–(2.8) was discussed in [48], see also [49]. In the following we derive a Lagrange multiplier type weak formulation of the system, which will be the basis for our finite element approximation. Let  $(\cdot, \cdot)_S$ ,  $S \subset \mathbf{R}^d$ , be the  $L^2(S)$  inner product and let  $\langle \cdot, \cdot \rangle_F$ ,  $F \subset \mathbf{R}^{d-1}$ , be the  $L^2(F)$  inner product or duality pairing. We will use the standard notation for Sobolev spaces, see, e.g. [14]. Let

$$\begin{aligned} \mathbf{V}_f &= \{\mathbf{v}_f \in H^1(\Omega_f)^d : \mathbf{v}_f = 0 \text{ on } \Gamma_f\}, & W_f &= L^2(\Omega_f), \\ \mathbf{V}_p &= \{\mathbf{v}_p \in H(\text{div}; \Omega_p) : \mathbf{v}_p \cdot \mathbf{n}_p = 0 \text{ on } \Gamma_p^N\}, & W_p &= L^2(\Omega_p), \\ \mathbf{X}_p &= \{\boldsymbol{\xi}_p \in H^1(\Omega_p)^d : \boldsymbol{\xi}_p = 0 \text{ on } \Gamma_p\}, & & \end{aligned} \quad (2.9)$$

where  $H(\text{div}; \Omega_p)$  is the space of  $L^2(\Omega_p)^d$ -vectors with divergence in  $L^2(\Omega_p)$  with a norm

$$\|\mathbf{v}\|_{H(\text{div}; \Omega_p)}^2 = \|\mathbf{v}\|_{L^2(\Omega_p)}^2 + \|\nabla \cdot \mathbf{v}\|_{L^2(\Omega_p)}^2.$$

We define the global velocity and pressure spaces as

$$\mathbf{V} = \{\mathbf{v} = (\mathbf{v}_f, \mathbf{v}_p) \in \mathbf{V}_f \times \mathbf{V}_p\}, \quad W = \{w = (w_f, w_p) \in W_f \times W_p\},$$

with norms

$$\|\mathbf{v}\|_{\mathbf{V}}^2 = \|\mathbf{v}_f\|_{H^1(\Omega_f)}^2 + \|\mathbf{v}_p\|_{H(\text{div}; \Omega_p)}^2, \quad \|w\|_W^2 = \|w_f\|_{L^2(\Omega_f)}^2 + \|w_p\|_{L^2(\Omega_p)}^2.$$

The weak formulation is obtained by multiplying the equations in each region by suitable test functions, integrating by parts the second order terms in space, and utilizing the interface and boundary conditions. Let

$$\begin{aligned} a_f(\mathbf{u}_f, \mathbf{v}_f) &= (2\mu \mathbf{D}(\mathbf{u}_f), \mathbf{D}(\mathbf{v}_f))_{\Omega_f}, \\ a_p^d(\mathbf{u}_p, \mathbf{v}_p) &= (\mu K^{-1} \mathbf{u}_p, \mathbf{v}_p)_{\Omega_p}, \\ a_p^e(\boldsymbol{\eta}_p, \boldsymbol{\xi}_p) &= (2\mu_p \mathbf{D}(\boldsymbol{\eta}_p), \mathbf{D}(\boldsymbol{\xi}_p))_{\Omega_p} + (\lambda_p \nabla \cdot \boldsymbol{\eta}_p, \nabla \cdot \boldsymbol{\xi}_p)_{\Omega_p} \end{aligned}$$

be the bilinear forms related to Stokes, Darcy and the elasticity operators, respectively. Let

$$b_\star(\mathbf{v}, w) = -(\nabla \cdot \mathbf{v}, w)_{\Omega_\star}.$$

Integration by parts in (2.1) and the two equations in (2.4) leads to the interface term

$$I_{\Gamma_{fp}} = -\langle \boldsymbol{\sigma}_f \mathbf{n}_f, \mathbf{v}_f \rangle_{\Gamma_{fp}} - \langle \boldsymbol{\sigma}_p \mathbf{n}_p, \boldsymbol{\xi}_p \rangle_{\Gamma_{fp}} + \langle p_p, \mathbf{v}_p \cdot \mathbf{n}_p \rangle_{\Gamma_{fp}}.$$

Using the first condition for balance of normal stress in (2.7) we set

$$\lambda = -(\boldsymbol{\sigma}_f \mathbf{n}_f) \cdot \mathbf{n}_f = p_p \text{ on } \Gamma_{fp},$$

which will be used as a Lagrange multiplier to impose the mass conservation interface condition (2.6). Utilizing the BJS condition (2.8) and the second condition for balance of stresses in (2.7), we obtain

$$I_{\Gamma_{fp}} = a_{BJS}(\mathbf{u}_f, \partial_t \boldsymbol{\eta}_p; \mathbf{v}_f, \boldsymbol{\xi}_p) + b_\Gamma(\mathbf{v}_f, \mathbf{v}_p, \boldsymbol{\xi}_p; \lambda),$$

where

$$a_{BJS}(\mathbf{u}_f, \boldsymbol{\eta}_p; \mathbf{v}_f, \boldsymbol{\xi}_p) = \sum_{j=1}^{d-1} \langle \mu \alpha_{BJS} \sqrt{K_j^{-1}} (\mathbf{u}_f - \boldsymbol{\eta}_p) \cdot \boldsymbol{\tau}_{f,j}, (\mathbf{v}_f - \boldsymbol{\xi}_p) \cdot \boldsymbol{\tau}_{f,j} \rangle_{\Gamma_{fp}},$$

$$b_\Gamma(\mathbf{v}_f, \mathbf{v}_p, \boldsymbol{\xi}_p; \mu) = \langle \mathbf{v}_f \cdot \mathbf{n}_f + (\boldsymbol{\xi}_p + \mathbf{v}_p) \cdot \mathbf{n}_p, \mu \rangle_{\Gamma_{fp}}.$$

For the well-posedness of  $b_\Gamma$  we require that  $\lambda \in \Lambda = (\mathbf{V}_p \cdot \mathbf{n}_p|_{\Gamma_{fp}})'$ . According to the normal trace theorem, since  $\mathbf{v}_p \in \mathbf{V}_p \subset H(\text{div}; \Omega_p)$ , then  $\mathbf{v}_p \cdot \mathbf{n}_p \in H^{-1/2}(\partial\Omega_p)$ . Furthermore, since  $\mathbf{v}_p \cdot \mathbf{n}_p = 0$  on  $\Gamma_p^N$  and  $\text{dist}(\Gamma_p^D, \Gamma_{fp}) \geq s > 0$ , then  $\mathbf{v}_p \cdot \mathbf{n}_p \in H^{-1/2}(\Gamma_{fp})$ , see, e.g. [23]. Therefore we take  $\Lambda = H^{1/2}(\Gamma_{fp})$ .

The Lagrange multiplier variational formulation is: for  $t \in (0, T]$ , find  $\mathbf{u}_f(t) \in \mathbf{V}_f$ ,  $p_f(t) \in W_f$ ,  $\mathbf{u}_p(t) \in \mathbf{V}_p$ ,  $p_p(t) \in W_p$ ,  $\boldsymbol{\eta}_p(t) \in \mathbf{X}_p$ , and  $\lambda(t) \in \Lambda$ , such that  $p_p(0) = p_{p,0}$ ,  $\boldsymbol{\eta}_p(0) = \boldsymbol{\eta}_{p,0}$ , and for all  $\mathbf{v}_f \in \mathbf{V}_f$ ,  $w_f \in W_f$ ,  $\mathbf{v}_p \in \mathbf{V}_p$ ,  $w_p \in W_p$ ,  $\boldsymbol{\xi}_p \in \mathbf{X}_p$ , and  $\mu \in \Lambda$ ,

$$a_f(\mathbf{u}_f, \mathbf{v}_f) + a_p^d(\mathbf{u}_p, \mathbf{v}_p) + a_p^e(\boldsymbol{\eta}_p, \boldsymbol{\xi}_p) + a_{BJS}(\mathbf{u}_f, \partial_t \boldsymbol{\eta}_p; \mathbf{v}_f, \boldsymbol{\xi}_p) + b_f(\mathbf{v}_f, p_f) + b_p(\mathbf{v}_p, p_p) + \alpha b_p(\boldsymbol{\xi}_p, p_p) + b_\Gamma(\mathbf{v}_f, \mathbf{v}_p, \boldsymbol{\xi}_p; \lambda) = (\mathbf{f}_f, \mathbf{v}_f)_{\Omega_f} + (\mathbf{f}_p, \boldsymbol{\xi}_p)_{\Omega_p}, \quad (2.10)$$

$$(s_0 \partial_t p_p, w_p)_{\Omega_p} - \alpha b_p(\partial_t \boldsymbol{\eta}_p, w_p) - b_p(\mathbf{u}_p, w_p) - b_f(\mathbf{u}_f, w_f) = (q_f, w_f)_{\Omega_f} + (q_p, w_p)_{\Omega_p}, \quad (2.11)$$

$$b_\Gamma(\mathbf{u}_f, \mathbf{u}_p, \partial_t \boldsymbol{\eta}_p; \mu) = 0. \quad (2.12)$$

where we used the notation  $\partial_t = \frac{\partial}{\partial t}$ . We note that the balance of normal stress, BJS, and conservation of momentum interface conditions (2.7)–(2.8) are natural and have been utilized in the derivation of the weak formulation, while the conservation of mass condition (2.6) is essential and it is imposed weakly in (2.12). The weak formulation (2.10)–(2.12) is suitable for multiscale numerical approximations and efficient parallel domain decomposition algorithms [2, 25, 27, 51].

### 3 Semi-discrete formulation

Let  $\mathcal{T}_h^f$  and  $\mathcal{T}_h^p$  be shape-regular and quasi-uniform partitions [14] of  $\Omega_f$  and  $\Omega_p$ , respectively, both consisting of affine elements with maximal element diameter  $h$ . The two partitions may be non-matching at the interface  $\Gamma_{fp}$ . For the discretization of the fluid velocity and pressure we choose finite element spaces  $\mathbf{V}_{f,h} \subset \mathbf{V}_f$  and  $W_{f,h} \subset W_f$ , which are assumed to be inf-sup stable. Examples of such spaces include the MINI elements, the Taylor-Hood elements and the conforming Crouzeix-Raviart elements. For the discretization of the porous medium problem we choose  $\mathbf{V}_{p,h} \subset \mathbf{V}_p$  and  $W_{p,h} \subset W_p$  to be any of well-known inf-sup stable mixed finite element spaces, such as the Raviart-Thomas or the Brezzi-Douglas-Marini spaces. The reader is referred to [7] for an overview of stable Stokes and Darcy mixed finite element spaces. The global spaces are

$$\mathbf{V}_h = \{\mathbf{v}_h = (\mathbf{v}_{f,h}, \mathbf{v}_{p,h}) \in \mathbf{V}_{f,h} \times \mathbf{V}_{p,h}\}, \quad W_h = \{w_h = (w_{f,h}, w_{p,h}) \in W_{f,h} \times W_{p,h}\}.$$

We employ a conforming Lagrangian finite element space  $\mathbf{X}_{p,h} \subset \mathbf{X}_h$  to approximate the structure displacement. Note that the finite element spaces  $\mathbf{V}_{f,h}$ ,  $\mathbf{V}_{p,h}$ , and  $\mathbf{X}_{p,h}$  satisfy the prescribed homogeneous boundary conditions on the external boundaries. For the discrete Lagrange multiplier space we take

$$\Lambda_h = \mathbf{V}_{p,h} \cdot \mathbf{n}_p|_{\Gamma_{fp}}.$$

The semi-discrete continuous-in-time problem reads: given  $p_{p,h}(0)$  and  $\boldsymbol{\eta}_{p,h}(0)$ , for  $t \in (0, T]$ , find  $\mathbf{u}_{f,h}(t) \in \mathbf{V}_{f,h}$ ,  $p_{f,h}(t) \in W_{f,h}$ ,  $\mathbf{u}_{p,h}(t) \in \mathbf{V}_{p,h}$ ,  $p_{p,h}(t) \in W_{p,h}$ ,  $\boldsymbol{\eta}_{p,h}(t) \in \mathbf{X}_{p,h}$ , and  $\lambda_h(t) \in \Lambda_h$  such that for all  $\mathbf{v}_{f,h} \in \mathbf{V}_{f,h}$ ,  $w_{f,h} \in W_{f,h}$ ,  $\mathbf{v}_{p,h} \in \mathbf{V}_{p,h}$ ,  $w_{p,h} \in W_{p,h}$ ,  $\boldsymbol{\xi}_{p,h} \in \mathbf{X}_{p,h}$ , and  $\mu_h \in \Lambda_h$ ,

$$\begin{aligned} a_f(\mathbf{u}_{f,h}, \mathbf{v}_{f,h}) + a_p^d(\mathbf{u}_{p,h}, \mathbf{v}_{p,h}) + a_p^e(\boldsymbol{\eta}_{p,h}, \boldsymbol{\xi}_{p,h}) + a_{BJS}(\mathbf{u}_{f,h}, \partial_t \boldsymbol{\eta}_{p,h}; \mathbf{v}_{f,h}, \boldsymbol{\xi}_{p,h}) + b_f(\mathbf{v}_{f,h}, p_{f,h}) \\ + b_p(\mathbf{v}_{p,h}, p_{p,h}) + \alpha b_p(\boldsymbol{\xi}_{p,h}, p_{p,h}) + b_\Gamma(\mathbf{v}_{f,h}, \mathbf{v}_{p,h}, \boldsymbol{\xi}_{p,h}; \lambda_h) = (\mathbf{f}_f, \mathbf{v}_{f,h})_{\Omega_f} + (\mathbf{f}_p, \boldsymbol{\xi}_{p,h})_{\Omega_p}, \end{aligned} \quad (3.1)$$

$$\begin{aligned} (s_0 \partial_t p_{p,h}, w_{p,h})_{\Omega_p} - \alpha b_p(\partial_t \boldsymbol{\eta}_{p,h}, w_{p,h}) - b_p(\mathbf{u}_{p,h}, w_{p,h}) - b_f(\mathbf{u}_{f,h}, w_{f,h}) \\ = (q_f, w_{f,h})_{\Omega_f} + (q_p, w_{p,h})_{\Omega_p}, \end{aligned} \quad (3.2)$$

$$b_\Gamma(\mathbf{u}_{f,h}, \mathbf{u}_{p,h}, \partial_t \boldsymbol{\eta}_{p,h}; \mu_h) = 0. \quad (3.3)$$

We will take  $p_{p,h}(0)$  and  $\boldsymbol{\eta}_{p,h}(0)$  to be suitable projections of the initial data  $p_{p,0}$  and  $\boldsymbol{\eta}_{p,0}$ .

The assumptions on the fluid viscosity  $\mu$  and the material coefficients  $K$ ,  $\lambda_p$ , and  $\mu_p$  imply that the bilinear forms  $a_f(\cdot, \cdot)$ ,  $a_p^d(\cdot, \cdot)$ , and  $a_p^e(\cdot, \cdot)$  are coercive and continuous in the appropriate norms. In particular, there exist positive constants  $c^f$ ,  $c^p$ ,  $c^e$ ,  $C^f$ ,  $C^p$ ,  $C^e$  such that

$$c^f \|\mathbf{v}_f\|_{H^1(\Omega_f)}^2 \leq a_f(\mathbf{v}_f, \mathbf{v}_f), \quad a_f(\mathbf{v}_f, \mathbf{q}_f) \leq C^f \|\mathbf{v}_f\|_{H^1(\Omega_f)} \|\mathbf{q}_f\|_{H^1(\Omega_f)}, \quad \forall \mathbf{v}_f, \mathbf{q}_f \in \mathbf{V}_f, \quad (3.4)$$

$$c^p \|\mathbf{v}_p\|_{L^2(\Omega_p)}^2 \leq a_p^d(\mathbf{v}_p, \mathbf{v}_p), \quad a_p^d(\mathbf{v}_p, \mathbf{q}_p) \leq C^p \|\mathbf{v}_p\|_{L^2(\Omega_p)} \|\mathbf{q}_p\|_{L^2(\Omega_p)}, \quad \forall \mathbf{v}_p, \mathbf{q}_p \in \mathbf{V}_p, \quad (3.5)$$

$$c^e \|\boldsymbol{\xi}_p\|_{H^1(\Omega_p)}^2 \leq a_p^e(\boldsymbol{\xi}_p, \boldsymbol{\xi}_p), \quad a_p^e(\boldsymbol{\xi}_p, \boldsymbol{\zeta}_p) \leq C^e \|\boldsymbol{\xi}_p\|_{H^1(\Omega_p)} \|\boldsymbol{\zeta}_p\|_{H^1(\Omega_p)}, \quad \forall \boldsymbol{\xi}_p, \boldsymbol{\zeta}_p \in \mathbf{X}_p, \quad (3.6)$$

where (3.4) and (3.6) hold true thanks to Poincaré inequality and (3.6) also relies on Korn's inequality, see [14] or [18] for more details. We further define, for  $\mathbf{v}_f \in \mathbf{V}_f$ ,  $\boldsymbol{\xi}_p \in \mathbf{X}_p$ ,

$$|\mathbf{v}_f - \boldsymbol{\xi}_p|_{a_{BJS}}^2 = a_{BJS}(\mathbf{v}_f, \boldsymbol{\xi}_p; \mathbf{v}_f, \boldsymbol{\xi}_p) = \sum_{j=1}^{d-1} \mu \alpha_{BJS} \|K_j^{-1/4} (\mathbf{v}_f - \boldsymbol{\xi}_p) \cdot \boldsymbol{\tau}_{f,j}\|_{L^2(\Gamma_{fp})}^2.$$

We next state a discrete inf-sup condition, which will be utilized to control the pressure in the two regions and the Lagrange multiplier. Following [23], we define a seminorm in  $\Lambda_h$ ,

$$|\mu_h|_{\Lambda_h}^2 = a_p^d(\mathbf{u}_{p,h}^*(\mu_h), \mathbf{u}_{p,h}^*(\mu_h)), \quad (3.7)$$

where  $(\mathbf{u}_{p,h}^*(\mu_h), p_{p,h}^*(\mu_h)) \in \mathbf{V}_{p,h} \times W_{p,h}$  is the mixed finite element solution to the Darcy problem with Dirichlet data  $\mu_h$  on  $\Gamma_{fp}$ :

$$\begin{aligned} a_p^d(\mathbf{u}_{p,h}^*(\mu_h), \mathbf{v}_{p,h}) + b_p(\mathbf{v}_{p,h}, p_{p,h}^*(\mu_h)) &= -\langle \mathbf{v}_{p,h} \cdot \mathbf{n}_p, \mu_h \rangle_{\Gamma_{fp}}, \quad \forall \mathbf{v}_{p,h} \in \mathbf{V}_{p,h}, \\ b_p(\mathbf{u}_{p,h}^*(\mu_h), w_{p,h}) &= 0, \quad \forall w_{p,h} \in W_{p,h}. \end{aligned}$$

We equip  $\Lambda_h$  with the norm  $\|\mu_h\|_{\Lambda_h}^2 = \|\mu_h\|_{L^2(\Gamma_{fp})}^2 + |\mu_h|_{\Lambda_h}^2$ . This norm can be considered as a discrete version of the  $H^{1/2}(\Gamma_{fp})$ -norm [23]. For convenience of notation we define the composite norms

$$\|(\mathbf{v}_h, \boldsymbol{\xi}_{p,h})\|_{\mathbf{V} \times \mathbf{X}_p}^2 = \|\mathbf{v}_h\|_{\mathbf{V}}^2 + \|\boldsymbol{\xi}_{p,h}\|_{H^1(\Omega_p)}^2, \quad \|(w_h, \mu_h)\|_{W \times \Lambda_h}^2 = \|w_h\|_W^2 + \|\mu_h\|_{\Lambda_h}^2,$$

as well as

$$\begin{aligned} b(\mathbf{v}_h, \boldsymbol{\xi}_{p,h}; w_h) &= b_f(\mathbf{v}_{f,h}, w_{f,h}) + b_p(\mathbf{v}_{p,h}, w_{p,h}) + \alpha b_p(\boldsymbol{\xi}_{p,h}, w_{p,h}), \\ b_\Gamma(\mathbf{v}_h, \boldsymbol{\xi}_{p,h}; \mu_h) &= b_\Gamma(\mathbf{v}_{f,h}, \mathbf{v}_{p,h}, \boldsymbol{\xi}_{p,h}; \mu_h). \end{aligned}$$

The next result establishes the Ladyzhenskaya-Babuska-Brezzi (LBB) condition for the mixed Stokes-Darcy problem, where it is understood that the zero functions are excluded from the inf-sup.

**Lemma 3.1.** *There exists a constant  $\beta > 0$  independent of  $h$  such that*

$$\inf_{(w_h, \mu_h) \in W_h \times \Lambda_h} \sup_{\mathbf{v}_h \in \mathbf{V}_h} \frac{b_f(\mathbf{v}_{f,h}; w_{f,h}) + b_p(\mathbf{v}_{p,h}; w_{p,h}) + \langle \mathbf{v}_{f,h} \cdot \mathbf{n}_f + \mathbf{v}_{p,h} \cdot \mathbf{n}_p, \mu_h \rangle}{\|\mathbf{v}_h\| \mathbf{V} \|(w_h, \mu_h)\|_{W \times \Lambda_h}} \geq \beta. \quad (3.8)$$

*Proof.* The result is proven in [23] in the case of velocity boundary conditions on  $\partial\Omega$  by restricting the mean value of  $W_h$ . It can be easily verified that, since  $|\Gamma_p^D| > 0$ , the result holds with no restriction on  $W_h$ .  $\square$

This result implies the inf-sup condition for the formulation (3.1)-(3.3).

**Corollary 3.1.** *There exists a constant  $\beta > 0$  independent of  $h$  such that*

$$\inf_{(w_h, \mu_h) \in W_h \times \Lambda_h} \sup_{(\mathbf{v}_h, \boldsymbol{\xi}_{p,h}) \in \mathbf{V}_h \times \mathbf{X}_{p,h}} \frac{b(\mathbf{v}_h, \boldsymbol{\xi}_{p,h}; w_h) + b_\Gamma(\mathbf{v}_h, \boldsymbol{\xi}_{p,h}; \mu_h)}{\|(\mathbf{v}_h, \boldsymbol{\xi}_{p,h})\| \mathbf{V} \times \mathbf{X}_p \|(w_h, \mu_h)\|_{W \times \Lambda_h}} \geq \beta. \quad (3.9)$$

*Proof.* The statement follows from Lemma 3.1 by simply taking  $\boldsymbol{\xi}_{p,h} = 0$ .  $\square$

### 3.1 Existence and uniqueness of the solution

In this section we show that the Stokes-Biot system is well-posed. For the existence of the solution we adopt the theory of differential-algebraic equations (DAEs) [8].

Let  $\{\phi_{\mathbf{u}_f,i}\}, \{\phi_{\mathbf{u}_p,i}\}, \{\phi_{\boldsymbol{\eta}_p,i}\}, \{\phi_{p_f,i}\}, \{\phi_{p_p,i}\}$  and  $\{\phi_{\lambda,i}\}$  be bases of  $\mathbf{V}_{f,h}, \mathbf{V}_{p,h}, \mathbf{X}_{p,h}, W_{f,h}, W_{p,h}$  and  $\Lambda_h$ , respectively. Let  $M_p, A_f, A_p, A_e, B_{ff}^T, B_{pp}^T$  and  $B_{ep}^T$  denote the matrices whose  $(i, j)$ -entries are, respectively,  $(\phi_{p_p,j}, \phi_{p_p,i})_{\Omega_p}$ ,  $a_f(\phi_{\mathbf{u}_f,j}, \phi_{\mathbf{u}_f,i})$ ,  $a_p^d(\phi_{\mathbf{u}_p,j}, \phi_{\mathbf{u}_p,i})$ ,  $a_p^e(\phi_{\boldsymbol{\eta}_p,j}, \phi_{\boldsymbol{\eta}_p,i})$ ,  $b_f(\nabla \cdot \phi_{\mathbf{u}_f,j}, \phi_{p_f,i})$ ,  $b_p(\nabla \cdot \phi_{\mathbf{u}_p,j}, \phi_{p_p,i})$ , and  $b_p(\nabla \cdot \phi_{\boldsymbol{\eta}_p,j}, \phi_{p_p,i})$ . We also introduce matrices  $A_{ff}^{BJS}, A_{fe}^{BJS}$  and  $A_{ee}^{BJS}$  whose  $(i, j)$ -entries are, respectively,  $a_{BJS}(\phi_{\mathbf{u}_f,j}, 0; \phi_{\mathbf{u}_f,i}, 0)$ ,  $a_{BJS}(\phi_{\mathbf{u}_f,j}, 0; 0, \phi_{\boldsymbol{\eta}_p,i})$ , and  $a_{BJS}(0, \phi_{\boldsymbol{\eta}_p,j}; 0, \phi_{\boldsymbol{\eta}_p,i})$ . Finally, let  $B_{f,\Gamma}^T, B_{p,\Gamma}^T$  and  $B_{e,\Gamma}^T$  stand for the matrices with  $(i, j)$ -entries defined by  $b_\Gamma(\phi_{\mathbf{u}_f,j}, 0, 0; \phi_{\lambda,i})$ ,  $b_\Gamma(0, \phi_{\mathbf{u}_p,j}, 0; \phi_{\lambda,i})$ , and  $b_\Gamma(0, 0, \phi_{\boldsymbol{\eta}_p,j}; \phi_{\lambda,i})$ , respectively.

Taking in (3.1)-(3.3)  $\mathbf{u}_{f,h}(t, \mathbf{x}) = \sum_i u_{f,i}(t) \phi_{\mathbf{u}_f,i}$ ,  $\mathbf{u}_{p,h}(t, \mathbf{x}) = \sum_i u_{p,i}(t) \phi_{\mathbf{u}_p,i}$ ,  $\boldsymbol{\eta}_{p,h}(t, \mathbf{x}) = \sum_i \eta_{p,i}(t) \phi_{\boldsymbol{\eta}_p,i}$ ,  $p_{f,h}(t, \mathbf{x}) = \sum_i p_{f,i}(t) \phi_{p_f,i}$ ,  $p_{p,h}(t, \mathbf{x}) = \sum_i p_{p,i}(t) \phi_{p_p,i}$  and  $\lambda_h(t, \mathbf{x}) = \sum_i \lambda_i(t) \phi_{\lambda,i}$  with (time-dependent) coefficients  $\bar{\mathbf{u}}_f, \bar{\mathbf{u}}_p, \bar{\boldsymbol{\eta}}_p, \bar{p}_f, \bar{p}_p, \bar{\lambda}$ , leads to the matrix-vector system

$$\begin{aligned} A_f \bar{\mathbf{u}}_f + A_p \bar{\mathbf{u}}_p + A_e \bar{\boldsymbol{\eta}}_p + A_{ff}^{BJS} \bar{\mathbf{u}}_f + A_{fe}^{BJS} \partial_t \bar{\boldsymbol{\eta}}_p + B_{ff}^T \bar{p}_f + (B_{pp}^T + \alpha B_{ep}^T) \bar{p}_p \\ + (B_{f,\Gamma}^T + B_{p,\Gamma}^T + B_{e,\Gamma}^T) \bar{\lambda} = \mathcal{F}_{\mathbf{u}_f} + \mathcal{F}_{\mathbf{u}_p} \end{aligned} \quad (3.10)$$

$$M_p \partial_t \bar{p}_p - \alpha B_{ep} \partial_t \bar{\boldsymbol{\eta}}_p - B_{pp} \bar{\mathbf{u}}_p - B_{ff} \bar{\mathbf{u}}_f + A_{fe}^{BJS,T} \bar{\mathbf{u}}_f + A_{ee}^{BJS} \partial_t \bar{\boldsymbol{\eta}}_p = \mathcal{F}_{p_f} + \mathcal{F}_{p_p}, \quad (3.11)$$

$$B_{f,\Gamma} \bar{\mathbf{u}}_f + B_{p,\Gamma} \bar{\mathbf{u}}_p + B_{e,\Gamma} \partial_t \bar{\boldsymbol{\eta}}_p = 0, \quad (3.12)$$

which can be written in the DAE system form

$$\mathbf{E} \partial_t X(t) + \mathbf{H} X(t) = L(t), \quad (3.13)$$

where

$$X(t) = \begin{pmatrix} \bar{\mathbf{u}}_f(t) \\ \bar{\mathbf{u}}_p(t) \\ \bar{\boldsymbol{\eta}}_p(t) \\ \bar{p}_f(t) \\ \bar{p}_p(t) \\ \bar{\lambda}(t) \end{pmatrix}, \quad L(t) = \begin{pmatrix} \mathcal{F}_{\mathbf{u}_f} \\ 0 \\ \mathcal{F}_{\boldsymbol{\eta}_p} \\ \mathcal{F}_{p_f} \\ \mathcal{F}_{p_p} \\ 0 \end{pmatrix}, \quad \mathbf{E} = \begin{pmatrix} 0 & 0 & A_{fe}^{BJS} & 0 & 0 & 0 \\ 0 & 0 & 0 & 0 & 0 & 0 \\ 0 & 0 & A_{ee}^{BJS} & 0 & 0 & 0 \\ 0 & 0 & 0 & 0 & 0 & 0 \\ 0 & 0 & -\alpha B_{ep} & 0 & s_0 M_p & 0 \\ 0 & 0 & -B_{e,\Gamma} & 0 & 0 & 0 \end{pmatrix}, \quad (3.14)$$

$$\mathbf{H} = \begin{pmatrix} A_f + A_{ff}^{BJS} & 0 & 0 & B_{ff}^T & 0 & B_{f,\Gamma}^T \\ 0 & A_p & 0 & 0 & B_{pp}^T & B_{p,\Gamma}^T \\ A_{fe}^{BJS,T} & 0 & A_e & 0 & \alpha B_{ep}^T & B_{e,\Gamma}^T \\ -B_{ff} & 0 & 0 & 0 & 0 & 0 \\ 0 & -B_{pp} & 0 & 0 & 0 & 0 \\ -B_{f,\Gamma} & -B_{p,\Gamma} & 0 & 0 & 0 & 0 \end{pmatrix}. \quad (3.15)$$

We note that the matrix

$$\mathbf{E} + \mathbf{H} = \begin{pmatrix} A_f + A_{ff}^{BJS} & 0 & A_{fe}^{BJS} & B_{ff}^T & 0 & B_{f,\Gamma}^T \\ 0 & A_p & 0 & 0 & B_{pp}^T & B_{p,\Gamma}^T \\ A_{fe}^{BJS,T} & 0 & A_e + A_{ee}^{BJS} & 0 & \alpha B_{ep}^T & B_{e,\Gamma}^T \\ -B_{ff} & 0 & 0 & 0 & 0 & 0 \\ 0 & -B_{pp} & -\alpha B_{ep} & 0 & s_0 M_p & 0 \\ -B_{f,\Gamma} & -B_{p,\Gamma} & -B_{e,\Gamma} & 0 & 0 & 0 \end{pmatrix}$$

can be written as a block  $2 \times 2$  matrix

$$\mathbf{E} + \mathbf{H} = \begin{pmatrix} \mathbf{A} & \mathbf{B}^T \\ -\mathbf{B} & \mathbf{C} \end{pmatrix},$$

where

$$\mathbf{A} = \begin{pmatrix} A_f + A_{ff}^{BJS} & 0 & A_{fe}^{BJS} \\ 0 & A_p & 0 \\ A_{fe}^{BJS,T} & 0 & A_e + A_{ee}^{BJS} \end{pmatrix}, \quad \mathbf{B}^T = \begin{pmatrix} B_{ff}^T & 0 & B_{f,\Gamma}^T \\ 0 & B_{pp}^T & B_{p,\Gamma}^T \\ 0 & \alpha B_{ep}^T & B_{e,\Gamma}^T \end{pmatrix}, \quad \mathbf{C} = \begin{pmatrix} 0 & 0 & 0 \\ 0 & s_0 M_p & 0 \\ 0 & 0 & 0 \end{pmatrix}.$$

The following result can be found in [54].



**Lemma 3.2.** *If  $\mathbf{A}$  and  $\mathbf{C}$  are positive semi-definite and  $\ker(\mathbf{A}) \cap \ker(\mathbf{B}) = \ker(\mathbf{C}) \cap \ker(\mathbf{B}^T) = \{0\}$ , then  $\mathbf{E} + \mathbf{H}$  is invertible.*

It is convenient to associate with matrices  $\mathbf{A}$ ,  $\mathbf{B}$ , and  $\mathbf{C}$  the bilinear forms  $\phi_{\mathbf{A}}(\cdot, \cdot)$ ,  $\phi_{\mathbf{B}}(\cdot, \cdot)$  and  $\phi_{\mathbf{C}}(\cdot, \cdot)$  on  $(\mathbf{V}_h \times \mathbf{X}_h) \times (\mathbf{V}_h \times \mathbf{X}_h)$ ,  $(\mathbf{V}_h \times \mathbf{X}_h) \times (W_h \times \Lambda_h)$  and  $(W_h \times \Lambda_h) \times (W_h \times \Lambda_h)$ , respectively:

$$\begin{aligned}\phi_{\mathbf{A}}((\mathbf{u}_h, \boldsymbol{\eta}_{p,h}), (\mathbf{v}_h, \boldsymbol{\xi}_{p,h})) &= a_f(\mathbf{u}_{f,h}, \mathbf{v}_{f,h}) + a_p^d(\mathbf{u}_{p,h}, \mathbf{v}_{p,h}) + a_p^e(\boldsymbol{\eta}_{p,h}, \boldsymbol{\xi}_{p,h}) \\ &\quad + a_{BJS}(\mathbf{u}_{f,h}, \boldsymbol{\eta}_{p,h}; \mathbf{v}_{v,h}, \boldsymbol{\xi}_{p,h}) \\ \phi_{\mathbf{B}}((\mathbf{u}_h, \boldsymbol{\eta}_{p,h}), (w_h, \mu_h)) &= b_f(\mathbf{u}_{f,h}, w_{f,h}) + b_p(\mathbf{u}_{p,h}, w_{p,h}) \\ &\quad + \alpha b_p(\boldsymbol{\eta}_{p,h}, w_{p,h}) + b_{\Gamma}(\mathbf{u}_{f,h}, \mathbf{u}_{p,h}, \boldsymbol{\eta}_{p,h}; \mu_h) \\ \phi_{\mathbf{C}}((p_h, \lambda_h), (w_h, \mu_h)) &= (s_0 p_{p,h}, w_{p,h})_{\Omega_p}.\end{aligned}$$

By identifying functions in the finite element spaces with algebraic vectors of their degrees of freedom, we note that  $\ker(\phi_{\mathbf{A}}) = \ker(\mathbf{A})$ ,  $\ker(\phi_{\mathbf{B}}) = \ker(\mathbf{B})$ , and  $\ker(\phi_{\mathbf{C}}) = \ker(\mathbf{C})$ . Also, for  $\phi_{\mathbf{B}^T}((w_h, \mu_h), (\mathbf{v}_h, \boldsymbol{\xi}_{p,h})) = \phi_{\mathbf{B}}((\mathbf{v}_h, \boldsymbol{\xi}_{p,h}), (w_h, \mu_h))$ , we have that  $\ker(\phi_{\mathbf{B}^T}) = \ker(\mathbf{B}^T)$ . We next show that the conditions of the Lemma 3.2 are satisfied.

**Lemma 3.3.** *The bilinear forms  $\phi_{\mathbf{A}}$ ,  $\phi_{\mathbf{B}}$  and  $\phi_{\mathbf{C}}$  satisfy*

$$\begin{aligned}\ker(\phi_{\mathbf{A}}) \cap \ker(\phi_{\mathbf{B}}) &= \{(0, 0)\}, \\ \ker(\phi_{\mathbf{C}}) \cap \ker(\phi_{\mathbf{B}^T}) &= \{(0, 0)\}.\end{aligned}$$

Moreover,  $\phi_{\mathbf{A}}$  and  $\phi_{\mathbf{C}}$  are positive definite and semi-definite, respectively.

*Proof.* The coercivity of  $a_f(\cdot, \cdot)$ ,  $a_p^d(\cdot, \cdot)$ , and  $a_p^e(\cdot, \cdot)$ , (3.4)–(3.6), and the non-negativity of  $a_{BJS}(\cdot, \cdot)$  imply that  $\phi_{\mathbf{A}}(\cdot, \cdot)$  is coercive and  $\ker(\phi_{\mathbf{A}}) = 0$ , hence the first statement of the lemma follows. We next note that  $\ker(\phi_{\mathbf{B}^T})$  consists of  $(w_h, \mu_h) \in W_h \times \Lambda_h$  such that

$$\phi_{\mathbf{B}^T}((w_h, \mu_h), (\mathbf{v}_h, \boldsymbol{\xi}_{p,h})) = 0, \quad \forall (\mathbf{v}_h, \boldsymbol{\xi}_{p,h}) \in \mathbf{V}_h \times \mathbf{X}_{p,h},$$

therefore the inf-sup condition (3.9) implies that  $\ker(\phi_{\mathbf{B}^T}) = \{(0, 0)\}$ , which gives the second statement of the lemma. The positive semi-definiteness of  $\phi_{\mathbf{C}}(\cdot, \cdot)$  is straightforward.  $\square$

To state the desired result, we will first introduce Bochner spaces equipped with norms:

$$\begin{aligned}\|\phi\|_{L^2(0,T;X)} &:= \left( \int_0^T \|\phi(t)\|_X^2 ds \right)^{1/2}, & \|\phi\|_{L^\infty(0,T;X)} &:= \operatorname{ess\,sup}_{t \in [0,T]} \|\phi(t)\|_X \\ \|\phi\|_{W^{1,\infty}(0,T;X)} &:= \operatorname{ess\,sup}_{t \in [0,T]} \{ \|\phi(t)\|_X, \|\partial_t \phi(t)\|_X \}.\end{aligned}\tag{3.16}$$

**Theorem 3.1.** *There exists a unique solution  $(\mathbf{u}_{f,h}, p_{f,h}, \mathbf{u}_{p,h}, p_{p,h}, \boldsymbol{\eta}_{p,h}, \lambda_h)$  in  $L^\infty(0, T; \mathbf{V}_{f,h}) \times L^\infty(0, T; W_{f,h}) \times L^\infty(0, T; \mathbf{V}_{p,h}) \times W^{1,\infty}(0, T; W_{p,h}) \times W^{1,\infty}(0, T; \mathbf{X}_{p,h}) \times L^\infty(0, T; \Lambda_h)$  of the weak formulation (3.1)–(3.3).*

*Proof.* According to the DAE theory, see Theorem 2.3.1 in [8], if the matrix pencil  $s\mathbf{E} + \mathbf{H}$  is nonsingular for some  $s \neq 0$  and the initial data is consistent, then (3.13) has a solution. Lemma 3.3 guarantees that in our case the pencil with  $s = 1$  is invertible. Also, the initial data  $p_{p,h}(0)$  and  $\boldsymbol{\eta}_{p,h}(0)$  does not lead to consistency issues. In particular, the only algebraic constraints in the DAE system (3.13) are the second and fourth equations, see the definition of  $\mathbf{E}$  in (3.14). The second equation is the discretized Darcy's law, and the initial value  $\mathbf{u}_{p,h}(0)$  can be chosen to satisfy it for any given  $p_{p,h}(0)$ , while the fourth

equation is the discretized incompressibility constraint for Stokes, which does not involve the initial data. Furthermore, the initial data can be assumed to satisfy the boundary conditions. As a result, Theorem 2.3.1 in [8] implies existence of a solution of the weak semi-discrete formulation (3.1)-(3.3).

To show uniqueness, we assume that there are two solutions satisfying these equations with the same initial conditions. Then their difference  $(\tilde{\mathbf{u}}_{f,h}, \tilde{p}_{f,h}, \tilde{\mathbf{u}}_{p,h}, \tilde{p}_{p,h}, \tilde{\boldsymbol{\eta}}_{p,h}, \tilde{\lambda}_h)$  satisfies (3.1)-(3.3) with zero data. By taking  $(\mathbf{v}_{f,h}, w_{f,h}, \mathbf{v}_{p,h}, w_{p,h}, \boldsymbol{\xi}_{p,h}, \mu_h) = (\tilde{\mathbf{u}}_{f,h}, \tilde{p}_{f,h}, \tilde{\mathbf{u}}_{p,h}, \tilde{p}_{p,h}, \partial_t \tilde{\boldsymbol{\eta}}_{p,h}, \tilde{\lambda}_h)$  in (3.1)-(3.3), we obtain the energy equality

$$a_f(\tilde{\mathbf{u}}_{f,h}, \tilde{\mathbf{u}}_{f,h}) + a_p^d(\tilde{\mathbf{u}}_{p,h}, \tilde{\mathbf{u}}_{p,h}) + a_p^e(\tilde{\boldsymbol{\eta}}_{p,h}, \partial_t \tilde{\boldsymbol{\eta}}_{p,h}) + (s_0 \partial_t \tilde{p}_{p,h}, \tilde{p}_{p,h}) + |\tilde{\mathbf{u}}_{f,h} - \partial_t \tilde{\boldsymbol{\eta}}_{p,h}|_{a_{BJS}}^2 = 0$$

Using the algebraic identity

$$\int_S \phi \frac{\partial \phi}{\partial t} = \frac{1}{2} \frac{\partial}{\partial t} \|\phi\|_{L^2(S)}^2 \quad (3.17)$$

we write the energy equality as

$$\frac{1}{2} \partial_t \left( s_0 \|\tilde{p}_{p,h}\|_{L^2(\Omega_p)}^2 + a_p^e(\tilde{\boldsymbol{\eta}}_{p,h}, \tilde{\boldsymbol{\eta}}_{p,h}) \right) + a_f(\tilde{\mathbf{u}}_{f,h}, \tilde{\mathbf{u}}_{f,h}) + a_p^d(\tilde{\mathbf{u}}_{p,h}, \tilde{\mathbf{u}}_{p,h}) + |\tilde{\mathbf{u}}_{f,h} - \partial_t \tilde{\boldsymbol{\eta}}_{p,h}|_{a_{BJS}}^2 = 0$$

Integrating in time over  $[0, t]$  for arbitrary  $t \in (0, T]$ , we obtain

$$\begin{aligned} & \frac{1}{2} \left( s_0 \|\tilde{p}_{p,h}(t)\|_{L^2(\Omega_p)}^2 + a_p^e(\tilde{\boldsymbol{\eta}}_{p,h}(t), \tilde{\boldsymbol{\eta}}_{p,h}(t)) \right) \\ & + \int_0^t \left[ |\tilde{\mathbf{u}}_{f,h} - \partial_t \tilde{\boldsymbol{\eta}}_{p,h}|_{a_{BJS}}^2 + a_f(\tilde{\mathbf{u}}_{f,h}, \tilde{\mathbf{u}}_{f,h}) + a_p^d(\tilde{\mathbf{u}}_{p,h}, \tilde{\mathbf{u}}_{p,h}) \right] ds = 0. \end{aligned} \quad (3.18)$$

Due to the coercivity of bilinear forms, we conclude that  $\tilde{\mathbf{u}}_{f,h}(t) = 0$ ,  $\tilde{\mathbf{u}}_{p,h}(t) = 0$ ,  $\tilde{\boldsymbol{\eta}}_{p,h}(t) = 0$ ,  $\forall t \in [0, T]$ . If  $s_0 \neq 0$ , we also have that  $\tilde{p}_{p,h}(t) = 0$ , but we can also obtain uniqueness for both pressure variables and the Lagrange multiplier simultaneously and independently of parameters. In particular, from the inf-sup condition (3.9) and (3.1), we have for  $(\tilde{p}_h, \tilde{\lambda}_h)$

$$\begin{aligned} \beta \|(\tilde{p}_h, \tilde{\lambda}_h)\|_{W \times \Lambda_h} & \leq \sup_{(\mathbf{v}_h, \boldsymbol{\xi}_{p,h}) \in \mathbf{V}_h \times \mathbf{X}_{p,h}} \frac{b_f(\mathbf{v}_{f,h}, \tilde{p}_{f,h}) + b_p(\mathbf{v}_{p,h}, \tilde{p}_{p,h}) + \alpha b_p(\boldsymbol{\xi}_{p,h}, \tilde{p}_{p,h}) + b_\Gamma(\mathbf{v}_{f,h}, \mathbf{v}_{p,h}, \boldsymbol{\xi}_{p,h}; \tilde{\lambda}_h)}{\|(\mathbf{v}_h, \boldsymbol{\xi}_h)\|_{\mathbf{V} \times \mathbf{X}_p}} \\ & = \sup_{(\mathbf{v}_h, \boldsymbol{\xi}_{p,h}) \in \mathbf{V}_h \times \mathbf{X}_{p,h}} \left[ \frac{-a_f(\tilde{\mathbf{u}}_{f,h}, \mathbf{v}_{f,h}) - a_p^d(\tilde{\mathbf{u}}_{p,h}, \mathbf{v}_{p,h}) - a_p^e(\tilde{\boldsymbol{\eta}}_{p,h}, \boldsymbol{\xi}_{p,h}) - a_{BJS}(\tilde{\mathbf{u}}_{f,h}, \partial_t \tilde{\boldsymbol{\eta}}_{p,h}; \mathbf{v}_{f,h}, \boldsymbol{\xi}_{p,h})}{\|(\mathbf{v}_h, \boldsymbol{\xi}_h)\|_{\mathbf{V} \times \mathbf{X}_p}} \right] = 0. \end{aligned}$$

Therefore, we conclude that  $\tilde{p}_{f,h}(t) = 0$ ,  $\tilde{p}_{p,h}(t) = 0$ ,  $\tilde{\lambda}_h(t) = 0$ ,  $\forall t \in (0, T]$  and the solution of (3.1)-(3.3) is unique.  $\square$

The next two sections are devoted to the stability and error analysis of the semi-discrete problem.

## 4 Stability analysis of the semi-discrete formulation

We will make use of the following well-known inequalities:

- (Cauchy-Schwarz) For any  $u, v \in L^2(S)$ ,

$$(u, v)_S \leq \|u\|_{L^2(S)} \|v\|_{L^2(S)}, \quad (4.1)$$

- (Trace) For any  $v \in H^1(S)$ ,

$$\|v\|_{L^2(\partial S)} \leq C\|v\|_{H^1(S)}, \quad (4.2)$$

- (Young's) For any real numbers  $a, b$  and  $\epsilon > 0$ ,

$$ab \leq \frac{\epsilon a^2}{2} + \frac{b^2}{2\epsilon}, \quad (4.3)$$

- (Gronwall's) Let  $g(t) \geq 0$  and  $u(t) \leq f(t) + \int_s^t g(\tau)u(\tau)d\tau$ , then

$$u(t) \leq f(t) + \int_s^t f(\tau)g(\tau) \exp\left(\int_\tau^t g(r)dr\right) d\tau. \quad (4.4)$$

For the sake of simplicity, throughout the analysis,  $C$  will denote a generic positive constant independent of the mesh size. We will also abuse notation by denoting  $\epsilon$  as an arbitrary constant with different values at different occurrences, arising from the usage of inequality (4.3).

By taking  $(\mathbf{v}_{f,h}, w_{f,h}, \mathbf{v}_{p,h}, w_{p,h}, \boldsymbol{\xi}_{p,h}, \mu_h) = (\mathbf{u}_{f,h}, p_{f,h}, \mathbf{u}_{p,h}, p_{p,h}, \partial_t \boldsymbol{\eta}_{p,h}, \lambda_h)$  in (3.1)–(3.3) and proceeding as in the uniqueness proof, Theorem 3.1, we obtain

$$\begin{aligned} & \frac{1}{2} \left( s_0 \|p_{p,h}(t)\|_{L^2(\Omega_p)}^2 + a_p^e(\boldsymbol{\eta}_{p,h}(t), \boldsymbol{\eta}_{p,h}(t)) \right) \\ & + \int_0^t \left[ \|\mathbf{u}_{f,h} - \partial_t \boldsymbol{\eta}_{p,h}\|_{a_{BJS}}^2 + a_f(\mathbf{u}_{f,h}, \mathbf{u}_{f,h}) + a_p^d(\mathbf{u}_{p,h}, \mathbf{u}_{p,h}) \right] ds \\ & = \frac{1}{2} \left( s_0 \|p_{p,h}(0)\|_{L^2(\Omega_p)}^2 + a_p^e(\boldsymbol{\eta}_{p,h}(0), \boldsymbol{\eta}_{p,h}(0)) \right) + \int_0^t \mathcal{F}(t; \mathbf{u}_{f,h}, \partial_t \boldsymbol{\eta}_{p,h}, p_{f,h}, p_{p,h}) ds, \end{aligned} \quad (4.5)$$

where  $\mathcal{F}(t; \mathbf{u}_{f,h}, \partial_t \boldsymbol{\eta}_{p,h}, p_{f,h}, p_{p,h})$  denotes the total forcing term:

$$\mathcal{F}(t; \mathbf{u}_{f,h}, \partial_t \boldsymbol{\eta}_{p,h}, p_{f,h}, p_{p,h}) = (\mathbf{f}_f, \mathbf{u}_{f,h})_{\Omega_f} + (\mathbf{f}_p, \partial_t \boldsymbol{\eta}_{p,h})_{\Omega_p} + (q_f, p_{f,h})_{\Omega_f} + (q_p, p_{p,h})_{\Omega_p}$$

Using integration by parts in time, we write the forcing term as

$$\mathcal{F}(t; \mathbf{u}_{f,h}, \partial_t \boldsymbol{\eta}_{p,h}, p_{f,h}, p_{p,h}) = (\mathbf{f}_f, \mathbf{u}_{f,h})_{\Omega_f} + \partial_t (\mathbf{f}_p, \boldsymbol{\eta}_{p,h})_{\Omega_p} - (\partial_t \mathbf{f}_p, \boldsymbol{\eta}_{p,h})_{\Omega_p} + (q_f, p_{f,h})_{\Omega_f} + (q_p, p_{p,h})_{\Omega_p}.$$

Therefore, for any  $\epsilon_1 > 0$ , we have

$$\begin{aligned} & \int_0^t \mathcal{F}(t; \mathbf{u}_{f,h}, \partial_t \boldsymbol{\eta}_{p,h}, p_{f,h}, p_{p,h}) ds \\ & \leq \frac{1}{2} \|\boldsymbol{\eta}_{p,h}(0)\|_{L^2(\Omega_p)}^2 + \frac{1}{2} \|\mathbf{f}_p(0)\|_{L^2(\Omega_p)}^2 + \frac{1}{2} \int_0^t \left( \|\boldsymbol{\eta}_{p,h}\|_{L^2(\Omega_p)}^2 + \|\partial_t \mathbf{f}_p\|_{L^2(\Omega_p)}^2 \right) ds \\ & \quad + \frac{\epsilon_1}{2} \left( \|\boldsymbol{\eta}_{p,h}(t)\|_{L^2(\Omega_p)}^2 + \int_0^t \left( \|\mathbf{u}_{f,h}\|_{L^2(\Omega_f)}^2 + \|p_{f,h}\|_{L^2(\Omega_f)}^2 + \|p_{p,h}\|_{L^2(\Omega_p)}^2 \right) ds \right) \\ & \quad + \frac{1}{2\epsilon_1} \left( \|\mathbf{f}_p(t)\|_{L^2(\Omega_p)}^2 + \int_0^t \left( \|\mathbf{f}_f\|_{L^2(\Omega_f)}^2 + \|q_f\|_{L^2(\Omega_f)}^2 + \|q_p\|_{L^2(\Omega_p)}^2 \right) ds \right). \end{aligned} \quad (4.6)$$

Combining (4.5), (4.6) and (3.4)–(3.6), and taking  $\epsilon_1$  small enough, we obtain

$$s_0 \|p_{p,h}(t)\|_{L^2(\Omega_p)}^2 + \|\boldsymbol{\eta}_{p,h}(t)\|_{H^1(\Omega_p)}^2 + \int_0^t \left( \|\mathbf{u}_{f,h} - \partial_t \boldsymbol{\eta}_{p,h}\|_{a_{BJS}}^2 + \|\mathbf{u}_{f,h}\|_{H^1(\Omega_f)}^2 + \|\mathbf{u}_{p,h}\|_{L^2(\Omega_p)}^2 \right) ds$$

$$\begin{aligned}
&\leq C\epsilon_1 \int_0^t \left( \|p_{f,h}\|_{L^2(\Omega_f)}^2 + \|p_{p,h}\|_{L^2(\Omega_p)}^2 \right) ds + C \int_0^t \|\boldsymbol{\eta}_{p,h}\|_{L^2(\Omega_p)}^2 ds \\
&\quad + C \left( s_0 \|p_{p,h}(0)\|_{L^2(\Omega_p)}^2 + \|\boldsymbol{\eta}_{p,h}(0)\|_{H^1(\Omega_p)}^2 + \|\mathbf{f}_p(0)\|_{L^2(\Omega_p)}^2 + \int_0^t \|\partial_t \mathbf{f}_p\|_{L^2(\Omega_p)}^2 ds \right) \\
&\quad + C\epsilon_1^{-1} \left( \|\mathbf{f}_p(t)\|_{L^2(\Omega_p)}^2 + \int_0^t \left( \|\mathbf{f}_f\|_{L^2(\Omega_f)}^2 + \|q_f\|_{L^2(\Omega_f)}^2 + \|q_p\|_{L^2(\Omega_p)}^2 \right) ds \right). \tag{4.7}
\end{aligned}$$

Finally, from the inf-sup condition (3.9) and (3.1), we have

$$\begin{aligned}
&\|(p_h, \lambda_h)\|_{W \times \Lambda_h} \\
&\leq C \sup_{(\mathbf{v}_h, \boldsymbol{\xi}_{p,h}) \in \mathbf{V}_h \times \mathbf{X}_{p,h}} \frac{b_f(\mathbf{v}_{f,h}, p_{f,h}) + b_p(\mathbf{v}_{p,h}, p_{p,h}) + \alpha b_p(\boldsymbol{\xi}_{p,h}, p_{p,h}) + b_\Gamma(\mathbf{v}_{f,h}, \mathbf{v}_{p,h}, \boldsymbol{\xi}_{p,h}; \lambda_h)}{\|(\mathbf{v}_h, \boldsymbol{\xi}_{p,h})\|_{\mathbf{V} \times \mathbf{X}_p}} \\
&= C \sup_{(\mathbf{v}_h, \boldsymbol{\xi}_{p,h}) \in \mathbf{V}_h \times \mathbf{X}_{p,h}} \left[ \frac{-a_f(\mathbf{u}_{f,h}, \mathbf{v}_{f,h}) - a_p^d(\mathbf{u}_{p,h}, \mathbf{v}_{p,h}) - a_p^e(\boldsymbol{\eta}_{p,h}, \boldsymbol{\xi}_{p,h})}{\|(\mathbf{v}_h, \boldsymbol{\xi}_{p,h})\|_{\mathbf{V} \times \mathbf{X}_p}} \right. \\
&\quad \left. + \frac{-a_{BJS}(\mathbf{u}_{f,h}, \partial_t \boldsymbol{\eta}_{p,h}; \mathbf{v}_{f,h}, \boldsymbol{\xi}_{p,h}) + (\mathbf{f}_f, \mathbf{v}_{f,h}) + (\mathbf{f}_p, \boldsymbol{\xi}_{p,h})}{\|(\mathbf{v}_h, \boldsymbol{\xi}_{p,h})\|_{\mathbf{V} \times \mathbf{X}_p}} \right],
\end{aligned}$$

which, combined with (3.4)–(3.6), gives

$$\begin{aligned}
\epsilon_2 \int_0^t \left( \|p_{f,h}\|_{L^2(\Omega_f)}^2 + \|p_{p,h}\|_{L^2(\Omega_p)}^2 + \|\lambda\|_{\Lambda_h}^2 \right) ds &\leq C\epsilon_2 \int_0^t \left( \|\mathbf{u}_{f,h}\|_{H^1(\Omega_f)}^2 + \|\mathbf{u}_{p,h}\|_{L^2(\Omega_p)}^2 + \|\boldsymbol{\eta}_{p,h}\|_{H^1(\Omega_p)}^2 \right. \\
&\quad \left. + |\mathbf{u}_{f,h} - \partial_t \boldsymbol{\eta}_{p,h}|_{a_{BJS}}^2 + \|\mathbf{f}_f\|_{L^2(\Omega_f)}^2 + \|\mathbf{f}_p\|_{L^2(\Omega_p)}^2 \right) ds. \tag{4.8}
\end{aligned}$$

Adding (4.7) and (4.8) and taking  $\epsilon_2$  small enough, and then  $\epsilon_1$  small enough, implies

$$\begin{aligned}
&s_0 \|p_{p,h}(t)\|_{L^2(\Omega_p)}^2 + \|\boldsymbol{\eta}_{p,h}(t)\|_{H^1(\Omega_p)}^2 + \int_0^t \left( |\mathbf{u}_{f,h} - \partial_t \boldsymbol{\eta}_{p,h}|_{a_{BJS}}^2 \right. \\
&\quad \left. + \|\lambda_h\|_{\Lambda_h}^2 + \|p_{f,h}\|_{L^2(\Omega_f)}^2 + \|p_{p,h}\|_{L^2(\Omega_p)}^2 + \|\mathbf{u}_f\|_{H^1(\Omega_f)}^2 + \|\mathbf{u}_p\|_{L^2(\Omega_p)}^2 \right) ds \\
&\leq C \left( \int_0^t \|\boldsymbol{\eta}_{p,h}\|_{H^1(\Omega_p)}^2 ds + s_0 \|p_{p,h}(0)\|_{L^2(\Omega_p)}^2 + \|\boldsymbol{\eta}_{p,h}(0)\|_{H^1(\Omega_p)}^2 + \|\mathbf{f}_p(0)\|_{L^2(\Omega_p)}^2 \right. \\
&\quad \left. + \int_0^t \left( \|\mathbf{f}_f\|_{L^2(\Omega_f)}^2 + \|\mathbf{f}_p\|_{L^2(\Omega_p)}^2 + \|\partial_t \mathbf{f}_p\|_{L^2(\Omega_p)}^2 + \|q_f\|_{L^2(\Omega_f)}^2 + \|q_p\|_{L^2(\Omega_p)}^2 \right) ds \right). \tag{4.9}
\end{aligned}$$

The use of Gronwall's inequality (4.4) implies the following stability result.

**Theorem 4.1.** *The solution of the semi-discrete problem (3.1)–(3.3) satisfies*

$$\begin{aligned}
&\sqrt{s_0} \|p_{p,h}\|_{L^\infty(0,T;L^2(\Omega_p))} + \|\boldsymbol{\eta}_{p,h}\|_{L^\infty(0,T;H^1(\Omega_p))} + \|\mathbf{u}_f\|_{L^2(0,T;H^1(\Omega_f))} + \|\mathbf{u}_p\|_{L^2(0,T;L^2(\Omega_p))} \\
&\quad + \|p_{f,h}\|_{L^2(0,T;L^2(\Omega_f))} + \|p_{p,h}\|_{L^2(0,T;L^2(\Omega_p))} + \|\lambda_h\|_{L^2(0,T;\Lambda_h)} + |\mathbf{u}_{f,h} - \partial_t \boldsymbol{\eta}_{p,h}|_{L^2(0,T;a_{BJS})} \\
&\leq C \sqrt{\exp(T)} \left( \sqrt{s_0} \|p_{p,h}(0)\|_{L^2(\Omega_p)} + \|\boldsymbol{\eta}_{p,h}(0)\|_{H^1(\Omega_p)} + \|\mathbf{f}_p\|_{L^\infty(0,T;L^2(\Omega_p))} + \|\mathbf{f}_p\|_{L^2(0,T;L^2(\Omega_p))} \right. \\
&\quad \left. + \|\mathbf{f}_f\|_{L^2(0,T;L^2(\Omega_f))} + \|\partial_t \mathbf{f}_p\|_{L^2(0,T;L^2(\Omega_p))} + \|q_f\|_{L^2(0,T;L^2(\Omega_f))} + \|q_p\|_{L^2(0,T;L^2(\Omega_p))} \right). \tag{4.10}
\end{aligned}$$

## 5 Error analysis

In this section, we analyze the error arising due to discretization in space. We denote by  $k_f$  and  $s_f$  the degrees of polynomials in the spaces  $\mathbf{V}_{f,h}$  and  $W_{f,h}$  respectively. Let  $k_p$  and  $s_p$  be the degrees of polynomials in the spaces  $\mathbf{V}_{p,h}$  and  $W_{p,h}$  respectively. Finally, let  $k_s$  be the polynomial degree in  $\mathbf{X}_{p,h}$ .

### 5.1 Approximation error

Let  $Q_{f,h}$ ,  $Q_{p,h}$ , and  $Q_{\lambda,h}$  be the  $L^2$ -projection operators onto  $W_{f,h}$ ,  $W_{p,h}$ , and  $\Lambda_h$  respectively, satisfying:

$$(p_f - Q_{f,h}p_f, w_{f,h})_{\Omega_f} = 0, \quad \forall w_{f,h} \in W_{f,h} \quad (5.1)$$

$$(p_p - Q_{p,h}p_p, w_{p,h})_{\Omega_p} = 0, \quad \forall w_{p,h} \in W_{p,h} \quad (5.2)$$

$$\langle \lambda - Q_{\lambda,h}\lambda, \mu_h \rangle_{\Gamma_{fp}} = 0, \quad \forall \mu_h \in \Lambda_h \quad (5.3)$$

These operators satisfy the approximation properties [14]:

$$\|p_f - Q_{f,h}p_f\|_{L^2(\Omega_f)} \leq Ch^{s_f+1} \|p_f\|_{H^{s_f+1}(\Omega_f)}, \quad (5.4)$$

$$\|p_p - Q_{p,h}p_p\|_{L^2(\Omega_p)} \leq Ch^{s_p+1} \|p_p\|_{H^{s_p+1}(\Omega_p)}, \quad (5.5)$$

$$\|\lambda - Q_{\lambda,h}\lambda\|_{L^2(\Gamma_{fp})} \leq Ch^{k_p+1} \|\lambda\|_{H^{k_p+1}(\Gamma_{fp})}. \quad (5.6)$$

Since the discrete Lagrange multiplier space is chosen as  $\Lambda_h = \mathbf{V}_{p,h} \cdot \mathbf{n}_p|_{\Gamma_{fp}}$ , we have

$$\langle \lambda - Q_{\lambda,h}\lambda, \mathbf{v}_{p,h} \cdot \mathbf{n}_p \rangle_{\Gamma_{fp}} = 0, \quad \forall \mathbf{v}_{p,h} \in \mathbf{V}_{p,h}.$$

We note that the discrete seminorm (3.7) in  $\Lambda_h$  is well defined for any function in  $L^2(\Gamma_{fp})$ . It is easy to see that  $|\lambda - Q_{\lambda,h}\lambda|_{\Lambda_h} = 0$ , hence

$$\|\lambda - Q_{\lambda,h}\lambda\|_{\Lambda_h} = \|\lambda - Q_{\lambda,h}\lambda\|_{L^2(\Gamma_{fp})}. \quad (5.7)$$

Next, we consider a Stokes-like projection operator  $(S_{f,h}, R_{f,h}) : \mathbf{V}_f \rightarrow \mathbf{V}_{f,h} \times W_{f,h}$ , defined for all  $\mathbf{v}_f \in \mathbf{V}_f$  by

$$a_f(S_{f,h}\mathbf{v}_f, \mathbf{v}_{f,h}) - b_f(\mathbf{v}_{f,h}, R_{f,h}\mathbf{v}_f) = a_f(\mathbf{v}_f, \mathbf{v}_{f,h}), \quad \forall \mathbf{v}_{f,h} \in \mathbf{V}_{f,h}, \quad (5.8)$$

$$b_f(S_{f,h}\mathbf{v}_f, w_{f,h}) = b_f(\mathbf{v}_f, w_{f,h}), \quad \forall w_{f,h} \in W_{f,h}. \quad (5.9)$$

The operator  $S_{f,h}$  satisfies the approximation property [19]:

$$\|\mathbf{v}_f - S_{f,h}\mathbf{v}_f\|_{H^1(\Omega_f)} \leq Ch^{k_f} \|\mathbf{v}_f\|_{H^{k_f+1}(\Omega_f)}. \quad (5.10)$$

Let  $\Pi_{p,h}$  be the MFE interpolant onto  $\mathbf{V}_{p,h}$  satisfying for any  $\theta > 0$  and for all  $\mathbf{v}_p \in \mathbf{V}_p \cap H^\theta(\Omega_p)$ ,

$$(\nabla \cdot \Pi_{p,h}\mathbf{v}_p, w_{p,h}) = (\nabla \cdot \mathbf{v}_p, w_{p,h}), \quad \forall w_{p,h} \in W_{p,h}, \quad (5.11)$$

$$\langle \Pi_{p,h}\mathbf{v}_p \cdot \mathbf{n}_p, \mathbf{v}_{p,h} \cdot \mathbf{n}_p \rangle_{\Gamma_{fp}} = \langle \mathbf{v}_p \cdot \mathbf{n}_p, \mathbf{v}_{p,h} \cdot \mathbf{n}_p \rangle_{\Gamma_{fp}}, \quad \forall \mathbf{v}_{p,h} \in \mathbf{V}_{p,h}. \quad (5.12)$$

We will make use of the following bounds on  $\Pi_{p,h}$  [14, 37]:

$$\|\mathbf{v}_p - \Pi_{p,h}\mathbf{v}_p\|_{L^2(\Omega_p)} \leq Ch^{k_p+1} \|\mathbf{v}_p\|_{H^{k_p+1}(\Omega_p)}, \quad (5.13)$$

$$\|\Pi_{p,h}\mathbf{v}_p\|_{H(\text{div}; \Omega_p)} \leq C \left( \|\mathbf{v}_p\|_{H^\theta(\Omega_p)} + \|\nabla \cdot \mathbf{v}_p\|_{L^2(\Omega_p)} \right). \quad (5.14)$$

Finally, let  $S_{s,h}$  be the Scott-Zhang interpolant onto  $\mathbf{X}_{p,h}$ , satisfying for all  $\boldsymbol{\xi}_p \in H^{k_s+1}(\Omega_p)$  [47]:

$$\|\boldsymbol{\xi}_p - S_{s,h}\boldsymbol{\xi}_p\|_{L^2(\Omega_p)} + h|\boldsymbol{\xi}_p - S_{s,h}\boldsymbol{\xi}_p|_{H^1(\Omega_p)} \leq Ch^{k_s+1} \|\boldsymbol{\xi}_p\|_{H^{k_s+1}(\Omega_p)} \quad (5.15)$$

### 5.1.1 Construction of a weakly-continuous interpolant

In this section we use the operators defined above to build an operator onto the space that satisfies the weak continuity of normal velocity condition (3.3). Let

$$\mathbf{U} = \{(\mathbf{v}_f, \mathbf{v}_p, \boldsymbol{\xi}_p) \in \mathbf{V}_f \times \mathbf{V}_p \cap H^0(\Omega_p) \times \mathbf{X}_p : \mathbf{v}_f \cdot \mathbf{n}_f + \mathbf{v}_p \cdot \mathbf{n}_p + \boldsymbol{\xi}_p \cdot \mathbf{n}_p = 0\}.$$

Consider its discrete analog

$$\mathbf{U}_h = \{(\mathbf{v}_{f,h}, \mathbf{v}_{p,h}, \boldsymbol{\xi}_{p,h}) \in \mathbf{V}_{f,h} \times \mathbf{V}_{p,h} \times \mathbf{X}_{p,h} : b_\Gamma(\mathbf{v}_{f,h}, \mathbf{v}_{p,h}, \boldsymbol{\xi}_{p,h}; \mu_h) = 0, \forall \mu_h \in \Lambda_h\}.$$

We will construct an interpolation operator  $I_h : \mathbf{U} \rightarrow \mathbf{U}_h$  as a triple

$$I_h(\mathbf{v}_f, \mathbf{v}_p, \boldsymbol{\xi}_p) = (I_{f,h}\mathbf{v}_f, I_{p,h}\mathbf{v}_p, I_{s,h}\boldsymbol{\xi}_p),$$

with the following properties:

$$b_\Gamma(I_{f,h}\mathbf{v}_f, I_{p,h}\mathbf{v}_p, I_{s,h}\boldsymbol{\xi}_p; \mu_h) = 0, \quad \forall \mu_h \in \Lambda_h, \quad (5.16)$$

$$b_f(I_{f,h}\mathbf{v}_f - \mathbf{v}_f, w_{f,h}) = 0, \quad \forall w_{f,h} \in W_{f,h}, \quad (5.17)$$

$$b_p(I_{p,h}\mathbf{v}_p - \mathbf{v}_p, w_{p,h}) = 0, \quad \forall w_{p,h} \in W_{p,h}. \quad (5.18)$$

We let  $I_{f,h} := S_{f,h}$  and  $I_{s,h} := S_{s,h}$ . To construct  $I_{p,h}$ , we first consider an auxiliary problem:

$$\begin{cases} \nabla \cdot \nabla \phi = 0 & \text{in } \Omega_p, \\ \phi = 0 & \text{on } \Gamma_p^D, \\ \nabla \phi \cdot \mathbf{n}_p = 0 & \text{on } \Gamma_p^N, \\ \nabla \phi \cdot \mathbf{n}_p = (\mathbf{v}_f - I_{f,h}\mathbf{v}_f) \cdot \mathbf{n}_f + (\boldsymbol{\xi}_p - I_{s,h}\boldsymbol{\xi}_p) \cdot \mathbf{n}_p & \text{on } \Gamma_{fp}. \end{cases} \quad (5.19)$$

Let  $\mathbf{z} = \nabla \phi$  and define  $\mathbf{w} = \mathbf{z} + \mathbf{v}_p$ . By construction,

$$\nabla \cdot \mathbf{w} = \nabla \cdot \mathbf{z} + \nabla \cdot \mathbf{v}_p = \nabla \cdot \mathbf{v}_p \quad \text{in } \Omega_p, \quad (5.20)$$

$$\begin{aligned} \mathbf{w} \cdot \mathbf{n}_p &= \mathbf{z} \cdot \mathbf{n}_p + \mathbf{v}_p \cdot \mathbf{n}_p = \mathbf{v}_f \cdot \mathbf{n}_f - I_{f,h}\mathbf{v}_f \cdot \mathbf{n}_f + \boldsymbol{\xi}_p \cdot \mathbf{n}_p - I_{s,h}\boldsymbol{\xi}_p \cdot \mathbf{n}_p + \mathbf{v}_p \cdot \mathbf{n}_p \\ &= -I_{f,h}\mathbf{v}_f \cdot \mathbf{n}_f - I_{s,h}\boldsymbol{\xi}_p \cdot \mathbf{n}_p \quad \text{on } \Gamma_{fp}. \end{aligned} \quad (5.21)$$

We now let

$$I_{p,h}\mathbf{v}_p = \Pi_{p,h}\mathbf{w}. \quad (5.22)$$

Next, we verify that the operator  $I_h = (I_{f,h}, I_{p,h}, I_{s,h})$  satisfies (5.16)–(5.18). Property (5.17) follows immediately from (5.9), while, using (5.11) and (5.20), property (5.18) follows from

$$(\nabla \cdot I_{p,h}\mathbf{v}_p, w_{p,h})_{\Omega_p} = (\nabla \cdot \Pi_{p,h}\mathbf{w}, w_{p,h})_{\Omega_p} = (\nabla \cdot \mathbf{w}, w_{p,h})_{\Omega_p} = (\nabla \cdot \mathbf{v}_p, w_{p,h})_{\Omega_p}, \quad \forall w_{p,h} \in W_{p,h}.$$

Using (5.21) and (5.12), we have for all  $\mu_h \in \Lambda_h$ ,

$$\langle I_{p,h}\mathbf{v}_p \cdot \mathbf{n}_p, \mu_h \rangle_{\Gamma_{fp}} = \langle \Pi_{p,h}\mathbf{w} \cdot \mathbf{n}_p, \mu_h \rangle_{\Gamma_{fp}} = \langle \mathbf{w} \cdot \mathbf{n}_p, \mu_h \rangle_{\Gamma_{fp}} = \langle -I_{f,h}\mathbf{v}_f \cdot \mathbf{n}_f - I_{s,h}\boldsymbol{\xi}_p \cdot \mathbf{n}_p, \mu_h \rangle_{\Gamma_{fp}},$$

which implies (5.16).

The approximation properties of the components of  $I_h$  are the following.

**Lemma 5.1.** For all  $(\mathbf{v}_f, \mathbf{v}_p, \boldsymbol{\xi}_p) \in \mathbf{U} \cap (H^{k_f+1}(\Omega_f), H^{k_p+1}(\Omega_p), H^{k_s+1}(\Omega_p))$ ,

$$\|\mathbf{v}_f - I_{f,h}\mathbf{v}_f\|_{H^1(\Omega_f)} \leq Ch^{k_f} \|\mathbf{v}_f\|_{H^{k_f+1}(\Omega_f)}, \quad (5.23)$$

$$\|\boldsymbol{\xi}_p - I_h^s \boldsymbol{\xi}_p\|_{H^m(\Omega_p)} \leq Ch^{k_s+1-m} \|\boldsymbol{\xi}_p\|_{H^{k_s+1}(\Omega_p)}, \quad m = 0, 1, \quad (5.24)$$

$$\|\mathbf{v}_p - I_{p,h}\mathbf{v}_p\|_{L^2(\Omega_p)} \leq C \left( h^{k_p+1} \|\mathbf{v}_p\|_{H^{k_p+1}(\Omega_p)} + h^{k_f} \|\mathbf{v}_f\|_{H^{k_f+1}(\Omega_f)} + h^{k_s} \|\boldsymbol{\xi}_p\|_{H^{k_s+1}(\Omega_p)} \right). \quad (5.25)$$

*Proof.* The bounds (5.23) and (5.24) follow immediately from (5.10) and (5.15). Next, using (5.22), we have

$$\|\mathbf{v}_p - I_{p,h}\mathbf{v}_p\|_{L^2(\Omega_p)} = \|\mathbf{v}_p - \Pi_{p,h}\mathbf{v}_p - \Pi_{p,h}\mathbf{z}\|_{L^2(\Omega_p)} \leq \|\mathbf{v}_p - \Pi_{p,h}\mathbf{v}_p\|_{L^2(\Omega_p)} + \|\Pi_{p,h}\mathbf{z}\|_{L^2(\Omega_p)}.$$

Elliptic regularity for (5.19) [29, 35] implies

$$\|\mathbf{z}\|_{H^\theta(\Omega_p)} \leq C \left( \|(\mathbf{v}_f - I_{f,h}\mathbf{v}_f) \cdot \mathbf{n}_f\|_{H^{\theta-1/2}(\Gamma_{fp})} + \|(\boldsymbol{\xi}_p - I_{s,h}\boldsymbol{\xi}_p) \cdot \mathbf{n}_p\|_{H^{\theta-1/2}(\Gamma_{fp})} \right), \quad 0 \leq \theta \leq 1/2.$$

Since  $\nabla \cdot \mathbf{z} = 0$  by construction, choosing  $\theta = 1/2$  and using (5.14), (4.2), (5.23) and (5.24), we get

$$\begin{aligned} \|\Pi_{p,h}\mathbf{z}\|_{L^2(\Omega_p)} &\leq C \|\mathbf{z}\|_{H^{1/2}(\Omega_p)} \\ &\leq C \left( \|(\mathbf{v}_f - I_{f,h}\mathbf{v}_f) \cdot \mathbf{n}_f\|_{L^2(\Gamma_{fp})} + \|(\boldsymbol{\xi}_p - I_{s,h}\boldsymbol{\xi}_p) \cdot \mathbf{n}_p\|_{L^2(\Gamma_{fp})} \right) \\ &\leq C \left( \|\mathbf{v}_f - I_{f,h}\mathbf{v}_f\|_{H^1(\Omega_f)} + \|\boldsymbol{\xi}_p - I_{s,h}\boldsymbol{\xi}_p\|_{H^1(\Omega_p)} \right) \\ &\leq C \left( h^{k_f} \|\mathbf{v}_f\|_{H^{k_f+1}(\Omega_f)} + h^{k_s} \|\boldsymbol{\xi}_p\|_{H^{k_s+1}(\Omega_p)} \right). \end{aligned}$$

Finally, by (5.13),

$$\begin{aligned} \|\mathbf{v}_p - I_{p,h}\mathbf{v}_p\|_{L^2(\Omega_p)} &\leq \|\mathbf{v}_p - \Pi_{p,h}\mathbf{v}_p\|_{L^2(\Omega_p)} + \|\Pi_{p,h}\mathbf{z}\|_{L^2(\Omega_p)} \\ &\leq C \left( h^{k_p+1} \|\mathbf{v}_p\|_{H^{k_p+1}(\Omega_p)} + h^{k_f} \|\mathbf{v}_f\|_{H^{k_f+1}(\Omega_f)} + h^{k_s} \|\boldsymbol{\xi}_p\|_{H^{k_s+1}(\Omega_p)} \right). \end{aligned}$$

□

## 5.2 Error estimates

In this section we derive a priori error estimate for the semi-discrete formulation (3.1)-(3.3). We recall that, due to (2.12),  $(\mathbf{u}_f, \mathbf{u}_p, \partial_t \boldsymbol{\eta}_p) \in \mathbf{U}$  and we can apply the interpolant  $I_h(\mathbf{u}_f, \mathbf{u}_p, \partial_t \boldsymbol{\eta}_p) = (I_{f,h}\mathbf{u}_f, I_{p,h}\mathbf{u}_p, I_{s,h}\partial_t \boldsymbol{\eta}_p) \in \mathbf{U}_h$  for any  $t \in (0, T]$ . We introduce the errors for all variables and split them into approximation and discretization errors:

$$\begin{aligned} \mathbf{e}_f &:= \mathbf{u}_f - \mathbf{u}_{f,h} = (\mathbf{u}_f - I_{f,h}\mathbf{u}_f) + (I_{f,h}\mathbf{u}_f - \mathbf{u}_{f,h}) := \boldsymbol{\chi}_f + \boldsymbol{\phi}_{f,h}, \\ \mathbf{e}_p &:= \mathbf{u}_p - \mathbf{u}_{p,h} = (\mathbf{u}_p - I_{p,h}\mathbf{u}_p) + (I_{p,h}\mathbf{u}_p - \mathbf{u}_{p,h}) := \boldsymbol{\chi}_p + \boldsymbol{\phi}_{p,h}, \\ \mathbf{e}_s &:= \boldsymbol{\eta}_p - \boldsymbol{\eta}_{p,h} = (\boldsymbol{\eta}_p - I_{s,h}\boldsymbol{\eta}_p) + (I_{s,h}\boldsymbol{\eta}_p - \boldsymbol{\eta}_{p,h}) := \boldsymbol{\chi}_s + \boldsymbol{\phi}_{s,h}, \\ e_{fp} &:= p_f - p_{f,h} = (p_f - Q_{f,h}p_f) + (Q_{f,h}p_f - p_{f,h}) := \chi_{fp} + \phi_{fp,h}, \\ e_{pp} &:= p_p - p_{p,h} = (p_p - Q_{p,h}p_p) + (Q_{p,h}p_p - p_{p,h}) := \chi_{pp} + \phi_{pp,h}, \\ e_\lambda &:= \lambda - \lambda_h = (\lambda - Q_{\lambda,h}\lambda) + (Q_{\lambda,h}\lambda - \lambda_h) := \chi_\lambda + \phi_{\lambda,h}. \end{aligned} \quad (5.26)$$

Subtracting (3.1)–(3.2) from (2.10)–(2.11) and summing the two equations, we obtain the error equation

$$\begin{aligned}
& a_f(\mathbf{e}_f, \mathbf{v}_{f,h}) + a_p^d(\mathbf{e}_p, \mathbf{v}_{p,h}) + a_p^e(\mathbf{e}_s, \boldsymbol{\xi}_{p,h}) + a_{BJS}(\mathbf{e}_f, \partial_t \mathbf{e}_s; \mathbf{v}_{f,h}, \boldsymbol{\xi}_{p,h}) + b_f(\mathbf{v}_{f,h}, e_{fp}) \\
& + b_p(\mathbf{v}_{p,h}, e_{pp}) + \alpha b_p(\boldsymbol{\xi}_{p,h}, e_{pp}) + b_\Gamma(\mathbf{v}_{f,h}, \mathbf{v}_{p,h}, \boldsymbol{\xi}_{p,h}; e_\lambda) + (s_0 \partial_t e_{pp}, w_{p,h}) \\
& - \alpha b_p(\partial_t e_s, w_{p,h}) - b_p(\mathbf{e}_p, w_{p,h}) - b_f(\mathbf{e}_f, w_{f,h}) = 0,
\end{aligned} \tag{5.27}$$

Setting  $\mathbf{v}_{f,h} = \boldsymbol{\phi}_{f,h}$ ,  $\mathbf{v}_{p,h} = \boldsymbol{\phi}_{p,h}$ ,  $\boldsymbol{\xi}_{p,h} = \partial_t \boldsymbol{\phi}_{s,h}$ ,  $w_{f,h} = \phi_{fp,h}$ , and  $w_{p,h} = \phi_{pp,h}$ , we have

$$\begin{aligned}
& a_f(\boldsymbol{\chi}_f, \boldsymbol{\phi}_{f,h}) + a_f(\boldsymbol{\phi}_{f,h}, \boldsymbol{\phi}_{f,h}) + a_p^d(\boldsymbol{\chi}_p, \boldsymbol{\phi}_{p,h}) + a_p^d(\boldsymbol{\phi}_{p,h}, \boldsymbol{\phi}_{p,h}) + a_p^e(\boldsymbol{\chi}_s, \partial_t \boldsymbol{\phi}_{s,h}) + a_p^e(\boldsymbol{\phi}_{s,h}, \partial_t \boldsymbol{\phi}_{s,h}) \\
& + a_{BJS}(\boldsymbol{\chi}_f, \partial_t \boldsymbol{\chi}_s; \boldsymbol{\phi}_{f,h}, \partial_t \boldsymbol{\phi}_{s,h}) + a_{BJS}(\boldsymbol{\phi}_{f,h}, \partial_t \boldsymbol{\phi}_{s,h}; \boldsymbol{\phi}_{f,h}, \partial_t \boldsymbol{\phi}_{s,h}) + b_f(\boldsymbol{\phi}_{f,h}, \chi_{fp}) + b_f(\boldsymbol{\phi}_{f,h}, \phi_{fp,h}) \\
& + b_p(\boldsymbol{\phi}_{p,h}, \chi_{pp}) + b_p(\boldsymbol{\phi}_{p,h}, \phi_{pp,h}) + \alpha b_p(\partial_t \boldsymbol{\phi}_{s,h}, \chi_{pp}) + \alpha b_p(\partial_t \boldsymbol{\phi}_{s,h}, \phi_{pp,h}) \\
& + b_\Gamma(\boldsymbol{\phi}_{f,h}, \boldsymbol{\phi}_{p,h}, \partial_t \boldsymbol{\phi}_{s,h}; \chi_\lambda) + b_\Gamma(\boldsymbol{\phi}_{f,h}, \boldsymbol{\phi}_{p,h}, \partial_t \boldsymbol{\phi}_{s,h}; \phi_{\lambda,h}) + (s_0 \partial_t \chi_{pp}, \phi_{pp,h}) + (s_0 \partial_t \phi_{pp,h}, \phi_{pp,h}) \\
& - \alpha b_p(\partial_t \boldsymbol{\chi}_s, \phi_{pp,h}) - \alpha b_p(\partial_t \boldsymbol{\phi}_{s,h}, \phi_{pp,h}) - b_p(\boldsymbol{\chi}_p, \phi_{pp,h}) - b_p(\boldsymbol{\phi}_{p,h}, \phi_{pp,h}) \\
& - b_f(\boldsymbol{\chi}_f, \phi_{fp,h}) - b_f(\boldsymbol{\phi}_{f,h}, \phi_{fp,h}) = 0.
\end{aligned} \tag{5.28}$$

The following terms simplify, due to the properties of projection operators (5.2), (5.3), (5.17), and (5.18):

$$b_f(\boldsymbol{\chi}_f, \phi_{fp,h}) = b_p(\boldsymbol{\chi}_p, \phi_{pp,h}) = b_p(\boldsymbol{\phi}_{p,h}, \chi_{pp}) = 0, \quad (s_0 \partial_t \chi_{pp}, \phi_{pp,h}) = \langle \boldsymbol{\phi}_{p,h} \cdot \mathbf{n}_p, \chi_\lambda \rangle_{\Gamma_{fp}} = 0, \tag{5.29}$$

where we also used that  $\Lambda_h = \mathbf{V}_{p,h} \cdot \mathbf{n}_p|_{\Gamma_{fp}}$  for the last equality. We also have

$$b_\Gamma(\boldsymbol{\phi}_{f,h}, \boldsymbol{\phi}_{p,h}, \partial_t \boldsymbol{\phi}_{s,h}; \phi_{\lambda,h}) = 0, \quad b_\Gamma(\boldsymbol{\phi}_{f,h}, \boldsymbol{\phi}_{p,h}, \partial_t \boldsymbol{\phi}_{s,h}; \chi_\lambda) = \langle \boldsymbol{\phi}_{f,h} \cdot \mathbf{n}_f + \partial_t \boldsymbol{\phi}_{s,h} \cdot \mathbf{n}_p, \chi_\lambda \rangle_{\Gamma_{fp}},$$

where we have used (5.16) and (3.3) for the first equality and the last equality in (5.29) for the second equality. Using (3.17), we write

$$(s_0 \partial_t \phi_{pp,h}, \phi_{pp,h}) = \frac{1}{2} s_0 \partial_t \|\phi_{pp,h}\|_{L^2(\Omega_p)}^2, \quad a_p^e(\boldsymbol{\phi}_{s,h}, \partial_t \boldsymbol{\phi}_{s,h}) = \frac{1}{2} \partial_t a_p^e(\boldsymbol{\phi}_{s,h}, \boldsymbol{\phi}_{s,h}).$$

Rearranging terms and using the results above, the error equation (5.28) becomes

$$\begin{aligned}
& a_f(\boldsymbol{\phi}_{f,h}, \boldsymbol{\phi}_{f,h}) + a_p^d(\boldsymbol{\phi}_{p,h}, \boldsymbol{\phi}_{p,h}) + \frac{1}{2} \partial_t \left( a_p^e(\boldsymbol{\phi}_{s,h}, \boldsymbol{\phi}_{s,h}) + s_0 \|\phi_{pp,h}\|_{L^2(\Omega_p)}^2 \right) + |\boldsymbol{\phi}_{f,h} - \partial_t \boldsymbol{\phi}_{s,h}|_{a_{BJS}}^2 \\
& = a_f(\boldsymbol{\chi}_f, \boldsymbol{\phi}_{f,h}) + a_p^d(\boldsymbol{\chi}_p, \boldsymbol{\phi}_{p,h}) + a_p^e(\boldsymbol{\chi}_s, \partial_t \boldsymbol{\phi}_{s,h}) \\
& + \sum_{j=1}^{d-1} \left\langle \mu \alpha_{BJS} \sqrt{K_j^{-1}} (\boldsymbol{\chi}_f - \partial_t \boldsymbol{\chi}_s) \cdot \boldsymbol{\tau}_{f,j}, (\boldsymbol{\phi}_{f,h} - \partial_t \boldsymbol{\phi}_{s,h}) \cdot \boldsymbol{\tau}_{f,j} \right\rangle_{\Gamma_{fp}} + b_f(\boldsymbol{\phi}_{f,h}, \chi_{fp}) \\
& + \alpha b_p(\partial_t \boldsymbol{\phi}_{s,h}, \chi_{pp}) + \alpha b_p(\partial_t \boldsymbol{\chi}_s, \phi_{pp,h}) + \langle \boldsymbol{\phi}_{f,h} \cdot \mathbf{n}_f + \partial_t \boldsymbol{\phi}_{s,h} \cdot \mathbf{n}_p, \chi_\lambda \rangle_{\Gamma_{fp}}.
\end{aligned} \tag{5.30}$$

We proceed with bounding the terms on the right-hand side in (5.30). Using the continuity of the bilinear forms (3.4) and (3.5) and inequalities (4.1) and (4.3), we have

$$a_f(\boldsymbol{\chi}_f, \boldsymbol{\phi}_{f,h}) + a_p^d(\boldsymbol{\chi}_p, \boldsymbol{\phi}_{p,h}) \leq C \epsilon_1^{-1} \left( \|\boldsymbol{\chi}_f\|_{H^1(\Omega_f)}^2 + \|\boldsymbol{\chi}_p\|_{L^2(\Omega_p)}^2 \right) + \epsilon_1 \left( \|\boldsymbol{\phi}_{f,h}\|_{H^1(\Omega_f)}^2 + \|\boldsymbol{\phi}_{p,h}\|_{L^2(\Omega_p)}^2 \right). \tag{5.31}$$

Similarly, using inequalities (4.1), (4.2) and (4.3), we obtain

$$\sum_{j=1}^{d-1} \left\langle \mu \alpha_{BJS} \sqrt{K_j^{-1}} (\boldsymbol{\chi}_f - \partial_t \boldsymbol{\chi}_s) \cdot \boldsymbol{\tau}_{f,j}, (\boldsymbol{\phi}_{f,h} - \partial_t \boldsymbol{\phi}_{s,h}) \cdot \boldsymbol{\tau}_{f,j} \right\rangle_{\Gamma_{fp}}$$



$$\leq \epsilon_1 |\phi_{f,h} - \partial_t \phi_{s,h}|_{a_{BJS}}^2 + C\epsilon_1^{-1} \left( \|\chi_f\|_{H^1(\Omega_f)}^2 + \|\partial_t \chi_s\|_{H^1(\Omega_p)}^2 \right). \quad (5.32)$$

Finally, using (4.1),(4.2) and (4.3), we bound the rest of the terms that do not involve  $\partial_t \phi_{s,h}$ :

$$\begin{aligned} & b_f(\phi_{f,h}, \chi_{fp}) + \alpha b_p(\partial_t \chi_s, \phi_{pp,h}) + \langle \phi_{f,h} \cdot \mathbf{n}_f, \chi_\lambda \rangle_{\Gamma_{fp}} \\ & \leq C\epsilon_1^{-1} \left( \|\chi_{fp}\|_{L^2(\Omega_f)}^2 + \|\nabla \cdot \partial_t \chi_s\|_{L^2(\Omega_p)}^2 + \|\chi_\lambda\|_{L^2(\Gamma_{fp})}^2 \right) \\ & \quad + \epsilon_1 \left( \|\nabla \cdot \phi_{f,h}\|_{L^2(\Omega_f)}^2 + \|\phi_{pp,h}\|_{L^2(\Omega_p)}^2 + \|\phi_{f,h} \cdot \mathbf{n}_f\|_{L^2(\Gamma_{fp})}^2 \right) \\ & \leq C\epsilon_1^{-1} \left( \|\chi_{fp}\|_{L^2(\Omega_f)}^2 + \|\partial_t \chi_s\|_{H^1(\Omega_p)}^2 + \|\chi_\lambda\|_{L^2(\Gamma_{fp})}^2 \right) + \epsilon_1 \left( \|\phi_{f,h}\|_{H^1(\Omega_f)}^2 + \|\phi_{pp,h}\|_{L^2(\Omega_p)}^2 \right). \end{aligned} \quad (5.33)$$

Combining (5.30)–(5.33), integrating over  $[0, t]$ , where  $0 < t \leq T$ , using the coercivity of the bilinear forms (3.4)–(3.6), and taking  $\epsilon_1$  small enough, we obtain

$$\begin{aligned} & \|\phi_{s,h}(t)\|_{H^1(\Omega_f)}^2 + s_0 \|\phi_{pp,h}(t)\|_{L^2(\Omega_p)}^2 + \|\phi_{f,h}\|_{L^2(0,t;H^1(\Omega_f))}^2 \\ & \quad + \|\phi_{p,h}\|_{L^2(0,t;L^2(\Omega_p))}^2 + \|\phi_{f,h} - \partial_t \phi_{s,h}\|_{L^2(0,t;a_{BJS})}^2 \\ & \leq \epsilon_1 \|\phi_{pp,h}\|_{L^2(0,t;L^2(\Omega_p))}^2 + C\epsilon_1^{-1} \left( \|\partial_t \chi_s\|_{L^2(0,t;H^1(\Omega_p))}^2 + \|\chi_{fp}\|_{L^2(0,t;L^2(\Omega_f))}^2 \right. \\ & \quad \left. + \|\chi_f\|_{L^2(0,t;H^1(\Omega_f))}^2 + \|\chi_p\|_{L^2(0,t;L^2(\Omega_p))}^2 + \|\chi_\lambda\|_{L^2(0,t;L^2(\Gamma_{fp}))}^2 \right) \\ & \quad + C \int_0^t (a_p^e(\chi_s, \partial_t \phi_{s,h}) + \alpha b_p(\partial_t \phi_{s,h}, \chi_{pp}) + \langle \partial_t \phi_{s,h} \cdot \mathbf{n}_p, \chi_\lambda \rangle_{\Gamma_{fp}}) ds \\ & \quad + C \left( \|\phi_{s,h}(0)\|_{H^1(\Omega_f)}^2 + s_0 \|\phi_{pp,h}(0)\|_{L^2(\Omega_p)}^2 \right). \end{aligned} \quad (5.34)$$

For the initial conditions, we set  $p_{p,h}(0) = Q_{p,h} p_{p,0}$  and  $\mathbf{n}_{p,h}(0) = I_{s,h} \mathbf{n}_{p,0}$ , implying

$$\phi_{s,h}(0) = 0, \quad \phi_{pp,h}(0) = 0 \quad (5.35)$$

We next bound the terms on the right involving  $\partial_t \phi_{s,h}$ . Using integration by parts in time, (4.1), (4.3), (3.6) and (5.35), we obtain

$$\begin{aligned} & \int_0^t a_p^e(\chi_s, \partial_t \phi_{s,h}) ds = a_p^e(\chi_s, \phi_{s,h})|_0^t - \int_0^t a_p^e(\partial_t \chi_s, \phi_{s,h}) ds \\ & \leq C \left( \epsilon_1^{-1} \|\chi_s(t)\|_{H^1(\Omega_p)}^2 + \|\partial_t \chi_s\|_{L^2(0,t;H^1(\Omega_p))}^2 \right) + \epsilon_1 \|\phi_{s,h}(t)\|_{H^1(\Omega_p)}^2 + \|\phi_{s,h}\|_{L^2(0,t;H^1(\Omega_p))}^2. \end{aligned} \quad (5.36)$$

Similarly, using (4.1), (4.2), (4.3) and (5.35), we have

$$\begin{aligned} & \int_0^t \langle \partial_t \phi_{s,h} \cdot \mathbf{n}_p, \chi_\lambda \rangle_{\Gamma_{fp}} ds + \int_0^t \alpha b_p(\partial_t \phi_{s,h}, \chi_{pp}) ds \\ & = \langle \phi_{s,h} \cdot \mathbf{n}_p, \chi_\lambda \rangle_{\Gamma_{fp}}|_0^t - \int_0^t \langle \phi_{s,h} \cdot \mathbf{n}_p, \partial_t \chi_\lambda \rangle_{\Gamma_{fp}} ds + \alpha b_p(\phi_{s,h}, \partial_t \chi_{pp})|_0^t - \int_0^t \alpha b_p(\phi_{s,h}, \partial_t \chi_{pp}) ds \\ & \leq \epsilon_1 \|\phi_{s,h}(t) \cdot \mathbf{n}_p\|_{L^2(\Gamma_{fp})}^2 + \|\phi_{s,h} \cdot \mathbf{n}_p\|_{L^2(0,t;L^2(\Gamma_{fp}))}^2 + \epsilon_1 \|\nabla \cdot \phi_{s,h}(t)\|_{L^2(\Omega_p)}^2 + \|\nabla \cdot \phi_{s,h}\|_{L^2(0,t;L^2(\Omega_p))}^2 \\ & \quad + C \left( \epsilon_1^{-1} \|\chi_\lambda(t)\|_{L^2(\Gamma_{fp})}^2 + \|\partial_t \chi_\lambda\|_{L^2(0,t;L^2(\Gamma_{fp}))}^2 + \epsilon_1^{-1} \|\chi_{pp}(t)\|_{L^2(\Omega_p)}^2 + \|\partial_t \chi_{pp}\|_{L^2(0,t;L^2(\Omega_p))}^2 \right) \\ & \leq \epsilon_1 \|\phi_{s,h}(t)\|_{H^1(\Omega_p)}^2 + \|\phi_{s,h}\|_{L^2(0,t;H^1(\Omega_p))}^2 \end{aligned}$$

$$+ C \left( \epsilon_1^{-1} \|\chi_\lambda(t)\|_{L^2(\Gamma_{fp})}^2 + \|\partial_t \chi_\lambda\|_{L^2(0,t;L^2(\Gamma_{fp}))}^2 + \epsilon_1^{-1} \|\chi_{pp}(t)\|_{L^2(\Omega_p)}^2 + \|\partial_t \chi_{pp}\|_{L^2(0,t;L^2(\Omega_p))}^2 \right). \quad (5.37)$$

Using (5.35)–(5.37) and taking  $\epsilon_1$  small enough, we obtain from (5.34),

$$\begin{aligned} & \|\phi_{s,h}(t)\|_{H^1(\Omega_p)}^2 + s_0 \|\phi_{pp,h}(t)\|_{L^2(\Omega_p)}^2 + \|\phi_{f,h}\|_{L^2(0,t;H^1(\Omega_f))}^2 \\ & \quad + \|\phi_{p,h}\|_{L^2(0,t;L^2(\Omega_p))}^2 + |\phi_{f,h} - \partial_t \phi_{s,h}|_{L^2(0,t;a_{BJS})}^2 \\ & \leq \epsilon_1 \|\phi_{pp,h}\|_{L^2(0,t;L^2(\Omega_p))}^2 + \|\phi_{s,h}\|_{L^2(0,t;H^1(\Omega_p))}^2 \\ & \quad + C \epsilon_1^{-1} \left( \|\chi_{fp}\|_{L^2(0,t;L^2(\Omega_f))}^2 + \|\chi_f\|_{L^2(0,t;H^1(\Omega_f))}^2 + \|\chi_p\|_{L^2(0,t;L^2(\Omega_p))}^2 \right. \\ & \quad \left. + \|\chi_\lambda(t)\|_{L^2(\Gamma_{fp})}^2 + \|\chi_{pp}(t)\|_{L^2(\Omega_p)}^2 + \|\chi_\lambda\|_{L^2(0,t;L^2(\Gamma_{fp}))}^2 + \|\chi_s(t)\|_{H^1(\Omega_p)}^2 \right) \\ & \quad + C \left( \|\partial_t \chi_s\|_{L^2(0,t;H^1(\Omega_p))}^2 + \|\partial_t \chi_\lambda\|_{L^2(0,t;L^2(\Gamma_{fp}))}^2 + \|\partial_t \chi_{pp}\|_{L^2(0,t;L^2(\Omega_p))}^2 \right). \end{aligned} \quad (5.38)$$

Next, we use the inf-sup condition (3.9) with the choice  $(w_h, \mu_h) = ((\phi_{fp,h}, \phi_{pp,h}), \phi_{\lambda,h})$  and the error equation obtained by subtracting (3.1) from (2.10):

$$\begin{aligned} & \|((\phi_{fp,h}, \phi_{pp,h}), \phi_{\lambda,h})\|_{W \times \Lambda_h} \\ & \leq C \sup_{(\mathbf{v}_h, \boldsymbol{\xi}_{p,h}) \in \mathbf{V}_h \times \mathbf{X}_{p,h}} \frac{b_f(\mathbf{v}_f, h, \phi_{fp,h}) + b_p(\mathbf{v}_p, h, \phi_{pp,h}) + \alpha b_p(\boldsymbol{\xi}_{p,h}, \phi_{pp,h}) + b_\Gamma(\mathbf{v}_f, h, \mathbf{v}_p, h, \boldsymbol{\xi}_{p,h}; \phi_{\lambda,h})}{\|(\mathbf{v}_h, \boldsymbol{\xi}_{p,h})\|_{\mathbf{V} \times \mathbf{X}_p}} \\ & = \sup_{(\mathbf{v}_h, \boldsymbol{\xi}_{p,h}) \in \mathbf{V}_h \times \mathbf{X}_{p,h}} \left( \frac{-a_f(\mathbf{e}_f, \mathbf{v}_f, h) - a_p^d(\mathbf{e}_p, \mathbf{v}_p, h) - a_p^e(\mathbf{e}_s, \boldsymbol{\xi}_{p,h}) - a_{BJS}(\mathbf{e}_f, \partial_t \mathbf{e}_s; \mathbf{v}_f, h, \boldsymbol{\xi}_{p,h})}{\|(\mathbf{v}_h, \boldsymbol{\xi}_{p,h})\|_{\mathbf{V} \times \mathbf{X}_p}} \right. \\ & \quad \left. + \frac{-b_f(\mathbf{v}_f, h, \chi_{fp}) - b_p(\mathbf{v}_p, h, \chi_{pp}) - \alpha b_p(\boldsymbol{\xi}_{p,h}, \chi_{pp}) - b_\Gamma(\mathbf{v}_f, h, \mathbf{v}_p, h, \boldsymbol{\xi}_{p,h}; \chi_\lambda)}{\|(\mathbf{v}_h, \boldsymbol{\xi}_{p,h})\|_{\mathbf{V} \times \mathbf{X}_p}} \right). \end{aligned}$$

Due to (5.2) and (5.3),  $b_p(\mathbf{v}_p, h, \chi_{pp}) = \langle \mathbf{v}_p, h \cdot \mathbf{n}_p, \chi_\lambda \rangle_{\Gamma_{fp}} = 0$ . Then, integrating over  $[0, t]$  and using the continuity of the bilinear forms (3.4)–(3.6) and the trace inequality (4.2), we get

$$\begin{aligned} & \epsilon_2 (\|\phi_{fp,h}\|_{L^2(0,t;L^2(\Omega_f))}^2 + \|\phi_{pp,h}\|_{L^2(0,t;L^2(\Omega_p))}^2 + \|\phi_{\lambda,h}\|_{L^2(0,t;L^2(\Gamma_{fp}))}^2) \\ & \leq C \epsilon_2 \left( \|\phi_{f,h}\|_{L^2(0,t;H^1(\Omega_f))}^2 + \|\phi_{p,h}\|_{L^2(0,t;L^2(\Omega_p))}^2 + \|\phi_{s,h}\|_{L^2(0,t;H^1(\Omega_p))}^2 + |\phi_{f,h} - \partial_t \phi_{s,h}|_{L^2(0,t;a_{BJS})}^2 \right. \\ & \quad + \|\chi_f\|_{L^2(0,t;H^1(\Omega_f))}^2 + \|\chi_p\|_{L^2(0,t;L^2(\Omega_p))}^2 + \|\partial_t \chi_s\|_{L^2(0,t;H^1(\Omega_p))}^2 \\ & \quad \left. + \|\chi_{fp}\|_{L^2(0,t;L^2(\Omega_f))}^2 + \|\chi_{pp}\|_{L^2(0,t;L^2(\Omega_p))}^2 + \|\chi_\lambda\|_{L^2(0,t;L^2(\Gamma_{fp}))}^2 \right). \end{aligned} \quad (5.39)$$

Adding (5.38) and (5.39) and taking  $\epsilon_2$  small enough, and then  $\epsilon_1$  small enough, gives

$$\begin{aligned} & \|\phi_{s,h}(t)\|_{H^1(\Omega_p)}^2 + s_0 \|\phi_{pp,h}(t)\|_{L^2(\Omega_p)}^2 + \|\phi_{f,h}\|_{L^2(0,t;H^1(\Omega_f))}^2 + \|\phi_{p,h}\|_{L^2(0,t;L^2(\Omega_p))}^2 \\ & \quad + |\phi_{f,h} - \partial_t \phi_{s,h}|_{L^2(0,t;a_{BJS})}^2 + \|\phi_{fp,h}\|_{L^2(0,t;L^2(\Omega_f))}^2 + \|\phi_{pp,h}\|_{L^2(0,t;L^2(\Omega_p))}^2 + \|\phi_{\lambda,h}\|_{L^2(0,t;\Lambda_h)}^2 \\ & \leq C \left( \|\phi_{s,h}\|_{L^2(0,t;H^1(\Omega_p))}^2 + \|\partial_t \chi_s\|_{L^2(0,t;H^1(\Omega_p))}^2 + \|\chi_{fp}\|_{L^2(0,t;L^2(\Omega_f))}^2 + \|\chi_f\|_{L^2(0,t;H^1(\Omega_f))}^2 \right. \\ & \quad + \|\chi_p\|_{L^2(0,t;L^2(\Omega_p))}^2 + \|\chi_\lambda(t)\|_{L^2(\Gamma_{fp})}^2 + \|\chi_{pp}(t)\|_{L^2(\Omega_p)}^2 + \|\chi_\lambda\|_{L^2(0,t;L^2(\Gamma_{fp}))}^2 + \|\partial_t \chi_\lambda\|_{L^2(0,t;L^2(\Gamma_{fp}))}^2 \\ & \quad \left. + \|\partial_t \chi_{pp}\|_{L^2(0,t;L^2(\Omega_p))}^2 + \|\partial_t \chi_s(t)\|_{H^1(\Omega_p)}^2 \right). \end{aligned} \quad (5.40)$$

Applying Gronwall's inequality (4.4) and using the triangle inequality and the approximation properties (5.4)–(5.6), (5.7) and (5.23)–(5.25), results in the following theorem.

**Theorem 5.1.** *Assuming sufficient smoothness for the solution of (2.10)–(2.12), then the solution of the semi-discrete problem (3.1)–(3.3) with  $p_{p,h}(0) = Q_{p,h}p_{p,0}$  and  $\boldsymbol{\eta}_{p,h}(0) = I_{s,h}\boldsymbol{\eta}_{p,0}$  satisfies*

$$\begin{aligned}
& \|\boldsymbol{\eta}_p - \boldsymbol{\eta}_{p,h}\|_{L^\infty(0,T;H^1(\Omega_p))} + \sqrt{s_0}\|p_p - p_{p,h}\|_{L^\infty(0,T;L^2(\Omega_p))} \\
& \quad + \|\mathbf{u}_f - \mathbf{u}_{f,h}\|_{L^2(0,T;H^1(\Omega_f))} + \|\mathbf{u}_p - \mathbf{u}_{p,h}\|_{L^2(0,T;L^2(\Omega_p))} + |(\mathbf{u}_f - \partial_t \boldsymbol{\eta}_p) - (\mathbf{u}_{f,h} - \partial_t \boldsymbol{\eta}_{p,h})|_{L^2(0,T; a_{BJS})} \\
& \quad + \|p_f - p_{f,h}\|_{L^2(0,T;L^2(\Omega_f))} + \|p_p - p_{p,h}\|_{L^2(0,T;L^2(\Omega_p))} + \|\lambda - \lambda_h\|_{L^2(0,T;\Lambda_h)} \\
& \leq C\sqrt{\exp(T)} \left( h^{k_f} \|\mathbf{u}_f\|_{L^2(0,T;H^{k_f+1}(\Omega_f))} + h^{s_f+1} \|p_f\|_{L^2(0,T;H^{s_f+1}(\Omega_f))} \right. \\
& \quad + h^{k_p+1} \left( \|\mathbf{u}_p\|_{L^2(0,T;H^{k_p+1}(\Omega_p))} + \|\lambda\|_{L^2(0,T;H^{k_p+1}(\Gamma_{fp}))} \right. \\
& \quad \quad \left. \left. + \|\lambda\|_{L^\infty(0,T;H^{k_p+1}(\Gamma_{fp}))} + \|\partial_t \lambda\|_{L^2(0,T;H^{k_p+1}(\Gamma_{fp}))} \right) \right. \\
& \quad + h^{s_p+1} \left( \|p_p\|_{L^\infty(0,T;H^{s_p+1}(\Omega_p))} + \|p_p\|_{L^2(0,T;H^{s_p+1}(\Omega_p))} + \|\partial_t p_p\|_{L^2(0,T;H^{s_p+1}(\Omega_p))} \right) \\
& \quad \left. + h^{k_s} \left( \|\boldsymbol{\eta}_p\|_{L^\infty(0,T;H^{k_s+1}(\Omega_p))} + \|\boldsymbol{\eta}_p\|_{L^2(0,T;H^{k_s+1}(\Omega_p))} + \|\partial_t \boldsymbol{\eta}_p\|_{L^2(0,T;H^{k_s+1}(\Omega_p))} \right) \right). \tag{5.41}
\end{aligned}$$

## 6 Fully discrete formulation

For the time discretization we employ the backward Euler method. Let  $\tau$  be the time step,  $T = N\tau$ , and let  $t_n = n\tau$ ,  $0 \leq n \leq N$ . Let  $d_\tau u^n := \tau^{-1}(u^n - u^{n-1})$  be the first order (backward) discrete time derivative, where  $u^n := u(t_n)$ . Then the fully discrete model reads: given  $p_{p,h}^0 = p_{p,h}(0)$  and  $\boldsymbol{\eta}_{p,h}^0 = \boldsymbol{\eta}_{p,h}(0)$ , find  $\mathbf{u}_{f,h}^n \in \mathbf{V}_{f,h}$ ,  $p_{f,h}^n \in W_{f,h}$ ,  $\mathbf{u}_{p,h}^n \in \mathbf{V}_{p,h}$ ,  $p_{p,h}^n \in W_{p,h}$ ,  $\boldsymbol{\eta}_{p,h}^n \in \mathbf{X}_{p,h}$ , and  $\lambda_h^n \in \Lambda_h$ ,  $1 \leq n \leq N$ , such that for all  $\mathbf{v}_{f,h} \in \mathbf{V}_{f,h}$ ,  $w_{f,h} \in W_{f,h}$ ,  $\mathbf{v}_{p,h} \in \mathbf{V}_{p,h}$ ,  $w_{p,h} \in W_{p,h}$ ,  $\boldsymbol{\xi}_{p,h} \in \mathbf{X}_{p,h}$ , and  $\mu_h \in \Lambda_h$ ,

$$\begin{aligned}
& a_f(\mathbf{u}_{f,h}^n, \mathbf{v}_{f,h}) + a_p^d(\mathbf{u}_{p,h}^n, \mathbf{v}_{p,h}) + a_p^e(\boldsymbol{\eta}_{p,h}^n, \boldsymbol{\xi}_{p,h}) + a_{BJS}(\mathbf{u}_{f,h}^n, d_\tau \boldsymbol{\eta}_{p,h}^n; \mathbf{v}_{f,h}, \boldsymbol{\xi}_{p,h}) + b_f(\mathbf{v}_{f,h}, p_{f,h}^n) \\
& \quad + b_p(\mathbf{v}_{p,h}, p_{p,h}^n) + \alpha b_p(\boldsymbol{\xi}_{p,h}, p_{p,h}^n) + b_\Gamma(\mathbf{v}_{f,h}, \mathbf{v}_{p,h}, \boldsymbol{\xi}_{p,h}; \lambda_h^n) = (\mathbf{f}_f^n, \mathbf{v}_{f,h})_{\Omega_f} + (\mathbf{f}_p^n, \boldsymbol{\xi}_{p,h})_{\Omega_p}, \tag{6.1}
\end{aligned}$$

$$\begin{aligned}
& (s_0 d_\tau p_{p,h}^n, w_{p,h})_{\Omega_p} - \alpha b_p(d_\tau \boldsymbol{\eta}_{p,h}^n, w_{p,h}) - b_p(\mathbf{u}_{p,h}^n, w_{p,h}) - b_f(\mathbf{u}_{f,h}^n, w_{f,h}) \\
& \quad = (q_f^n, w_{f,h})_{\Omega_f} + (q_p^n, w_{p,h})_{\Omega_p}, \tag{6.2}
\end{aligned}$$

$$b_\Gamma(\mathbf{u}_{f,h}^n, \mathbf{u}_{p,h}^n, d_\tau \boldsymbol{\eta}_{p,h}^n; \mu_h) = 0. \tag{6.3}$$

We introduce the discrete-in-time norms

$$\|\phi\|_{l^2(0,T;X)}^2 := \left( \tau \sum_{n=1}^N \|\phi^n\|_X^2 \right)^{1/2}, \quad \|\phi\|_{l^\infty(0,T;X)} := \max_{0 \leq n \leq N} \|\phi^n\|_X.$$

Next, we state the main results for the formulation (6.1)–(6.3). The proofs follow the framework in the semi-discrete case. Details can be found in the Appendix.

**Theorem 6.1.** *The solution of fully discrete problem (6.1)–(6.3) satisfies*

$$\sqrt{s_0}\|p_{p,h}\|_{l^\infty(0,T;L^2(\Omega_p))} + \|\boldsymbol{\eta}_{p,h}\|_{l^\infty(0,T;H^1(\Omega_p))} + \|\mathbf{u}_{f,h}\|_{l^2(0,T;H^1(\Omega_f))} + \|\mathbf{u}_{p,h}\|_{l^2(0,T;L^2(\Omega_p))}$$

$$\begin{aligned}
& + |\mathbf{u}_{f,h} - d_\tau \boldsymbol{\eta}_{p,h}|_{L^2(0,T;a_{BJS})} + \|p_{p,h}\|_{L^2(0,T;L^2(\Omega_p))} + \|p_{f,h}\|_{L^2(0,T;L^2(\Omega_f))} + \|\lambda_h\|_{L^2(0,T;\Lambda_h)} \\
& + \tau \left( \sqrt{s_0} \|d_\tau p_{p,h}\|_{L^2(0,T;L^2(\Omega_p))} + \|d_\tau \boldsymbol{\eta}_{p,h}\|_{L^2(0,T;H^1(\Omega_p))} \right) \\
\leq & C \sqrt{\exp(T)} \left( \sqrt{s_0} \|p_{p,h}^0\|_{L^2(\Omega_p)} + \|\boldsymbol{\eta}_{p,h}^0\|_{H^1(\Omega_p)} + \|\mathbf{f}_p\|_{L^\infty(0,T;L^2(\Omega_p))} + \|\partial_t \mathbf{f}_p\|_{L^2(0,T;L^2(\Omega_p))} \right. \\
& \left. + \|\mathbf{f}_f\|_{L^2(0,T;L^2(\Omega_f))} + \|q_f\|_{L^2(0,T;L^2(\Omega_f))} + \|q_p\|_{L^2(0,T;L^2(\Omega_p))} + \|\mathbf{f}_p\|_{L^2(0,T;L^2(\Omega_p))} \right).
\end{aligned}$$

**Theorem 6.2.** *Assuming sufficient smoothness for the solution of (2.10)–(2.12), then the solution of the fully discrete problem (6.1)–(6.3) satisfies*

$$\begin{aligned}
& \sqrt{s_0} \|p_p - p_{p,h}\|_{L^\infty(0,T;L^2(\Omega_p))} + \|\boldsymbol{\eta} - \boldsymbol{\eta}_{p,h}\|_{L^\infty(0,T;H^1(\Omega_p))} \\
& + \sqrt{\tau} \left( \sqrt{s_0} \|d_\tau(p_p - p_{p,h})\|_{L^2(0,T;L^2(\Omega_p))} + \|d_\tau(\boldsymbol{\eta}_p - \boldsymbol{\eta}_{p,h})\|_{L^2(0,T;H^1(\Omega_p))} \right) \\
& + \left( \|\mathbf{u}_f - \mathbf{u}_{f,h}\|_{L^2(0,T;H^1(\Omega_f))} + \|\mathbf{u}_p - \mathbf{u}_{p,h}\|_{L^2(0,T;L^2(\Omega_p))} + |\mathbf{u}_f - d_\tau \boldsymbol{\eta}_p - (\mathbf{u}_{f,h} - d_\tau \boldsymbol{\eta}_{p,h})|_{L^2(0,T;a_{BJS})} \right. \\
& \left. + \|p_f - p_{f,h}\|_{L^2(0,T;L^2(\Omega_f))} + \|p_p - p_{p,h}\|_{L^2(0,T;L^2(\Omega_p))} + \|\lambda - \lambda_h\|_{L^2(0,T;\Lambda_h)} \right) \\
\leq & C \sqrt{\exp(T)} \left( h^{k_f} \|\mathbf{u}_f\|_{L^2(0,T;H^{k_f+1}(\Omega_f))} + h^{s_f+1} \|p_f\|_{L^2(0,T;H^{s_f+1}(\Omega_f))} \right. \\
& + h^{k_p+1} \left( \|\mathbf{u}_p\|_{L^2(0,T;H^{k_p+1}(\Omega_p))} + \|\lambda\|_{L^2(0,T;H^{k_p+1}(\Gamma_{fp}))} + \|\lambda\|_{L^\infty(0,T;H^{k_p+1}(\Gamma_{fp}))} + \|\partial_t \lambda\|_{L^2(0,T;H^{k_p+1}(\Omega_p))} \right) \\
& + h^{s_p+1} \left( \|p_p\|_{L^2(0,T;H^{k_p+1}(\Omega_p))}^2 + \|p_p\|_{L^\infty(0,T;H^{s_p+1}(\Omega_p))} + \|\partial_t p_p\|_{L^2(0,T;H^{s_p+1}(\Omega_p))} \right) \\
& + h^{k_s} \left( \|\boldsymbol{\eta}_p\|_{L^2(0,T;H^{k_s+1}(\Omega_p))} + \|\boldsymbol{\eta}_p\|_{L^\infty(0,T;H^{k_s+1}(\Omega_p))} + \|\partial_t \boldsymbol{\eta}_p\|_{L^2(0,T;H^{k_s+1}(\Omega_p))} \right) \\
& \left. + \tau \left( \sqrt{s_0} \|\partial_{tt} p_p\|_{L^2(0,T;L^2(\Omega_p))} + \|\partial_{tt} \boldsymbol{\eta}_p\|_{L^2(0,T;H^1(\Omega_p))} \right) \right).
\end{aligned}$$

## 7 Numerical results

In this section, we present results from several computational experiments in two dimensions. The fully discrete method (6.1)–(6.3) has been implemented using the finite element package FreeFem++ [30]. The first test confirms the theoretical convergence rates for the problem using an analytical solution. The second and third examples show the applicability of the method to modeling fluid flow in an irregularly shaped fractured reservoir with physical parameters, while the last one performs a sensitivity analysis for the method with respect to various parameters.

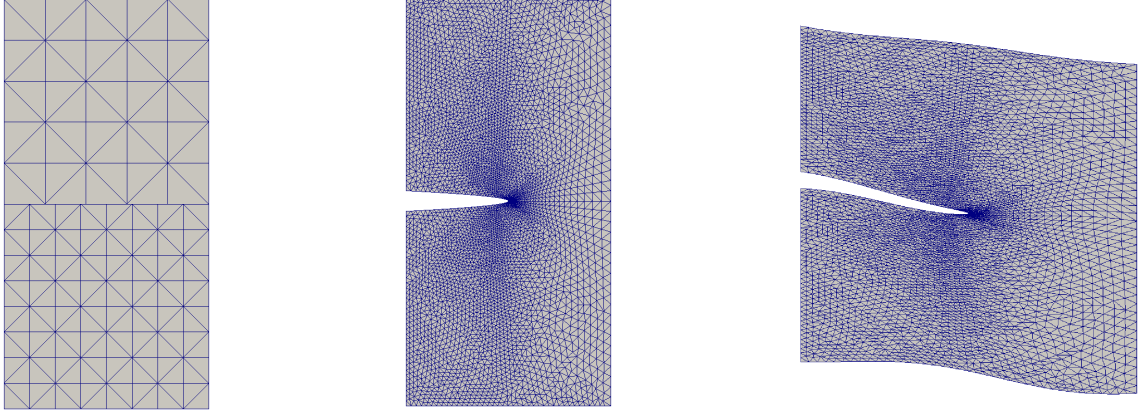
### 7.1 Convergence test

In this test we study the convergence for the space discretization using an analytical solution. The domain is  $\Omega = [0, 1] \times [-1, 1]$ , see Figure 1a. We associate the upper half with the Stokes flow, while the lower half represents the flow in the poroelastic structure governed by the Biot system. The appropriate interface conditions are enforced along the interface  $y = 0$ . The solution in the Stokes region is

$$\mathbf{u}_f = \pi \cos(\pi t) \begin{pmatrix} -3x + \cos(y) \\ y + 1 \end{pmatrix}, \quad p_f = \mathbf{e}^t \sin(\pi x) \cos\left(\frac{\pi y}{2}\right) + 2\pi \cos(\pi t).$$

The Biot solution is chosen accordingly to satisfy the interface conditions (2.6)–(2.8):

$$\mathbf{u}_p = \pi \mathbf{e}^t \begin{pmatrix} \cos(\pi x) \cos\left(\frac{\pi y}{2}\right) \\ \frac{1}{2} \sin(\pi x) \sin\left(\frac{\pi y}{2}\right) \end{pmatrix}, \quad p_p = \mathbf{e}^t \sin(\pi x) \cos\left(\frac{\pi y}{2}\right), \quad \boldsymbol{\eta}_p = \sin(\pi t) \begin{pmatrix} -3x + \cos(y) \\ y + 1 \end{pmatrix}.$$



(a) Computational domain  $\Omega$  in Example 1, non-matching grids    (b) Reference domain  $\hat{\Omega}$  in Examples 2, 3, and 4    (c) Physical domain  $\Omega$  in Examples 2 and 4

Figure 1: Simulation domains.

The right hand side functions  $\mathbf{f}_f$ ,  $q_f$ ,  $\mathbf{f}_p$  and  $q_p$  are computed from (2.1)–(2.5) using the above solution. The model problem is then complemented with the appropriate Dirichlet boundary conditions and initial data. The total simulation time for this test case is  $T = 0.01$ s and the time step is  $\Delta t = 10^{-3}$ s. The time step is sufficiently small, so that the time discretization error does not affect the convergence rates.

We study the convergence for two choices of finite element spaces. The lower order choice is the MINI elements [3]  $\mathcal{P}_1^b - \mathcal{P}_1$  for Stokes, the Raviart-Thomas [44]  $\mathcal{RT}_0 - \mathcal{P}_0$  and continuous Lagrangian  $\mathcal{P}_1$  elements for the Biot system, and piecewise constant Lagrange multiplier  $\mathcal{P}_0$ . In this case  $k_f = 1$ ,  $s_f = 1$ ,  $k_p = 0$ ,  $s_p = 0$ , and  $k_s = 1$ , so Theorem 6.2 implies first order of convergence for all variables. The higher order choice is the Taylor-Hood [50]  $\mathcal{P}_2 - \mathcal{P}_1$  for Stokes, the Raviart-Thomas  $\mathcal{RT}_1 - \mathcal{P}_1^{dc}$  and  $\mathcal{P}_2$  for Biot, and  $\mathcal{P}_1^{dc}$  for the Lagrange multiplier, with  $k_f = 2$ ,  $s_f = 1$ ,  $k_p = 1$ ,  $s_p = 1$ , and  $k_s = 2$ , in which case second order convergence rate for all variables is expected. These theoretical results are verified by the rates shown in the Table 1, where the errors were computed on a sequence of refined meshes, which are matching along the interface.

We also perform a convergence test with the lower order choice of finite elements on non-matching grids along the interface. We prescribe the ratio between mesh characteristic sizes to be  $h_{Stokes} = \frac{5}{8}h_{Biot}$  as shown in Figure 1a. According to the results shown in Table 2, first order convergence is observed for all variables, which agrees with Theorem 6.2.

## 7.2 Application to flow through fractured reservoirs

For the rest of the cases, we introduce the reference domain  $\hat{\Omega}$  given by the rectangle  $[0, 1] \times [-1, 1]$ m, see Figure 1b. A fracture, which represents the reference fluid domain  $\hat{\Omega}_f$  is then positioned in the middle of the rectangle, with the boundary defined by

$$\hat{x}^2 = 200(0.05 - \hat{y})(0.05 + \hat{y}), \quad \hat{y} \in [-0.05, 0.05].$$

| $\mathcal{P}_1^b - \mathcal{P}_1, \mathcal{RT}_0 - \mathcal{P}_0, \mathcal{P}_1$ and $\mathcal{P}_0$         |   |      |                                   |      |   |      |  |      |  |      |
|--|---|------|-----------------------------------|------|---|------|--|------|--|------|
| $h$  | $\ \mathbf{e}_f\ _{l^2(H^1(\Omega_f))}$ |      | $\ e_{fp}\ _{l^2(L^2(\Omega_f))}$ |      | $\ \mathbf{e}_p\ _{l^2(L^2(\Omega_p))}$ |      | $\ e_{pp}\ _{l^\infty(L^2(\Omega_p))}$ |      | $\ \mathbf{e}_s\ _{l^\infty(H_1(\Omega_p))}$ |      |
|  | error                                   | rate | error                             | rate | error                                   | rate | error                                  | rate | error  | rate |
| 1/8  | 8.96E-03                                | –    | 2.61E-03                          | –    | 1.05E-01                                | –    | 1.03E-01                               | –    | 5.09E-02                                     | –    |
| 1/16   | 4.47E-03                                | 1.0  | 8.33E-04                          | 1.6  | 5.23E-02                                | 1.0  | 5.17E-02                               | 1.0  | 1.34E-02                                     | 1.9  |
| 1/32   | 2.24E-03                                | 1.0  | 2.76E-04                          | 1.6  | 2.61E-02                                | 1.0  | 2.59E-02                               | 1.0  | 3.94E-03                                     | 1.8  |
| 1/64   | 1.12E-03                                | 1.0  | 9.43E-05                          | 1.6  | 1.31E-02                                | 1.0  | 1.29E-02                               | 1.0  | 1.43E-03                                     | 1.5  |
| 1/128  | 5.59E-04                                | 1.0  | 3.28E-05                          | 1.5  | 6.53E-03                                | 1.0  | 6.47E-03                               | 1.0  | 6.32E-04                                     | 1.2  |
| $\mathcal{P}_2 - \mathcal{P}_1, \mathcal{RT}_1 - \mathcal{P}_1^{dc}, \mathcal{P}_2$ and $\mathcal{P}_1^{dc}$ |   |      |                                   |      |   |      |  |      |  |      |
| $h$  | $\ \mathbf{e}_f\ _{l^2(H^1(\Omega_f))}$ |      | $\ e_{fp}\ _{l^2(L^2(\Omega_f))}$ |      | $\ \mathbf{e}_p\ _{l^2(L^2(\Omega_p))}$ |      | $\ e_{pp}\ _{l^\infty(L^2(\Omega_p))}$ |      | $\ \mathbf{e}_s\ _{l^\infty(H_1(\Omega_p))}$ |      |
|  | error                                   | rate | error                             | rate | error                                   | rate | error                                  | rate | error  | rate |
| 1/8  | 1.25E-04                                | –    | 1.31E-03                          | –    | 1.82E-02                                | –    | 1.60E-02                               | –    | 1.54E-01                                     | –    |
| 1/16   | 2.90E-05                                | 2.1  | 3.25E-04                          | 2.0  | 4.38E-03                                | 2.1  | 4.01E-03                               | 2.0  | 3.82E-02                                     | 2.0  |
| 1/32   | 7.06E-06                                | 2.0  | 8.07E-05                          | 2.0  | 1.08E-03                                | 2.0  | 1.00E-03                               | 2.0  | 9.51E-03                                     | 2.0  |
| 1/64   | 1.77E-06                                | 2.0  | 1.97E-05                          | 2.0  | 2.67E-04                                | 2.0  | 2.51E-04                               | 2.0  | 2.37E-03                                     | 2.0  |
| 1/128  | 4.73E-07                                | 1.9  | 4.51E-06                          | 2.1  | 6.47E-05                                | 2.0  | 6.23E-05                               | 2.0  | 5.89E-04                                     | 2.0  |

Table 1: Example 1: relative numerical errors and convergence rates on matching grids.

| $\mathcal{P}_1^b - \mathcal{P}_1, \mathcal{RT}_0 - \mathcal{P}_0, \mathcal{P}_1$ and $\mathcal{P}_0$ |   |      |                                   |      |   |      |  |      |  |      |
|--|---|------|-----------------------------------|------|---|------|--|------|--|------|
| $h_{Biot}$   | $\ \mathbf{e}_f\ _{l^2(H^1(\Omega_f))}$ |      | $\ e_{fp}\ _{l^2(L^2(\Omega_f))}$ |      | $\ \mathbf{e}_p\ _{l^2(L^2(\Omega_p))}$ |      | $\ e_{pp}\ _{l^\infty(L^2(\Omega_p))}$ |      | $\ \mathbf{e}_s\ _{l^\infty(H_1(\Omega_p))}$ |      |
|  | error                                   | rate | error                             | rate | error                                   | rate | error                                  | rate | error  | rate |
| 1/8  | 1.43E-02                                | –    | 6.06E-03                          | –    | 1.05E-01                                | –    | 1.03E-01                               | –    | 5.09E-02                                     | –    |
| 1/16   | 7.16E-03                                | 1.0  | 1.79E-03                          | 1.8  | 5.23E-02                                | 1.0  | 5.17E-02                               | 1.0  | 1.34E-02                                     | 1.9  |
| 1/32   | 3.58E-03                                | 1.0  | 5.81E-04                          | 1.6  | 2.61E-02                                | 1.0  | 2.59E-02                               | 1.0  | 3.94E-03                                     | 1.8  |
| 1/64   | 1.79E-03                                | 1.0  | 1.95E-04                          | 1.6  | 1.31E-02                                | 1.0  | 1.29E-02                               | 1.0  | 1.43E-03                                     | 1.5  |
| 1/128  | 8.94E-04                                | 1.0  | 6.77E-05                          | 1.5  | 6.53E-03                                | 1.0  | 6.47E-03                               | 1.0  | 6.32E-04                                     | 1.2  |

Table 2: Example 1: relative numerical errors and convergence rates on non-matching grids.

Furthermore, the physical domain  $\Omega$ , see Figure 1c, with more realistic geometry, is defined as a transformation of the reference domain  $\hat{\Omega}$  by the mapping [9]

$$\begin{bmatrix} x \\ y \end{bmatrix} = \begin{bmatrix} \hat{x} \\ 5 \cos(\frac{\hat{x}+\hat{y}}{100}) \cos(\frac{\pi\hat{x}+\hat{y}}{100})^2 + \hat{y}/2 - \hat{x}/10 \end{bmatrix}.$$

The external boundary of  $\Omega_f$  is denoted as  $\Gamma_{f,inflow}$ , while the external boundary of  $\Omega_p$  is split into  $\Gamma_{p,\star}$ , where  $\star \in \{left, right, top, bottom\}$ .

The next example is focused on modeling the interaction between a stationary fracture filled with fluid and the surrounding poroelastic reservoir. We are interested in the solution on the physical domain  $\Omega$ . The physical units are meters for length, seconds for time, and KPa for pressure. The boundary

conditions are chosen to be

$$\begin{array}{llll}
\text{Injection:} & \mathbf{u}_f \cdot \mathbf{n}_f = 10, & \mathbf{u}_f \cdot \boldsymbol{\tau}_f = 0 & \text{on } \Gamma_{f,inflow}, \\
\text{No flow:} & \mathbf{u}_p \cdot \mathbf{n}_p = 0 & & \text{on } \Gamma_{p,left}, \\
\text{Pressure:} & p_p = 1000 & & \text{on } \Gamma_{p,bottom} \cup \Gamma_{p,right} \cup \Gamma_{p,top}, \\
\text{Normal displacement:} & \boldsymbol{\eta}_p \cdot \mathbf{n}_p = 0 & & \text{on } \Gamma_{p,top} \cup \Gamma_{p,right} \cup \Gamma_{p,bottom}, \\
\text{Shear traction:} & (\boldsymbol{\sigma}_p \mathbf{n}_p) \cdot \boldsymbol{\tau}_p = 0 & & \text{on } \Gamma_{p,top} \cup \Gamma_{p,right} \cup \Gamma_{p,bottom}.
\end{array}$$

The initial conditions are set accordingly to  $\boldsymbol{\eta}_p(0) = 0$  m and  $p_p(0) = 10^3$  KPa. The total simulation time is  $T = 300$  s and the time step is  $\Delta t = 1$  s. The model parameters are given in Table 3. These parameters are realistic for hydraulic fracturing and are similar to the ones used in [28]. The Lamé coefficients are determined from the Young’s modulus  $E$  and the Poisson’s ratio  $\nu$  via the relationships  $\lambda_p = E\nu/[(1 + \nu)(1 - 2\nu)]$ ,  $\mu_p = E/[2(1 + \nu)]$ . We note that this is a challenging computational test due to the large variation in parameter values.

For this and the rest of the test cases we use the Taylor-Hood  $\mathcal{P}_2 - \mathcal{P}_1$  [50] elements for the fluid velocity and pressure in the fracture region, the Raviart-Thomas  $\mathcal{RT}_1 - \mathcal{P}_1^{dc}$  elements for the Darcy velocity and pressure, the continuous Lagrangian  $\mathcal{P}_1$  elements for the structure displacement, and the  $\mathcal{P}_1^{dc}$  elements for the Lagrange multiplier.

| Parameter                          | Symbol         | Units                | Values                          |
|------------------------------------|----------------|----------------------|---------------------------------|
| Young’s modulus                    | $E$            | (KPa)                | $10^7$                          |
| Poisson’s ratio                    | $\nu$          |                      | 0.2                             |
| Lamé coefficient                   | $\lambda_p$    | (KPa)                | $5/18 \times 10^7$              |
| Lamé coefficient                   | $\mu_p$        | (KPa)                | $5/12 \times 10^7$              |
| Dynamic viscosity                  | $\mu$          | (KPa s)              | $10^{-6}$                       |
| Permeability                       | $K$            | (m <sup>2</sup> )    | $diag(200, 50) \times 10^{-12}$ |
| Mass storativity                   | $s_0$          | (KPa <sup>-1</sup> ) | $6.89 \times 10^{-2}$           |
| Biot-Willis constant               | $\alpha$       |                      | 1.0                             |
| Beavers-Joseph-Saffman coefficient | $\alpha_{BJS}$ |                      | 1.0                             |
| Total time                         | T              | (s)                  | 300                             |

Table 3: Poroelasticity and fluid parameters in Example 2.

Figure 2 shows the structure (top) and fracture (bottom) regions for the described test case at the final time  $T = 300$  s. The grayscale velocity legend in Figure 2a is included to show the range of the Darcy velocity magnitude. We observe channel-like flow in the fracture region, which concentrates at the tip, and leak-off into the reservoir. The fluid pressure in the reservoir has increased in the vicinity of the fracture from the initial value of 1000 KPa to approximately 2450 KPa, which is close to the pressure in the fracture. The pressure drop in the reservoir in the direction away from the fracture is significant, but the resulting Darcy velocity is relatively small, due to the very low permeability. The displacement field shows that the fracture tends to open as the fluid is being injected, with the deformation of the rock being largest around the fracture and quickly approaching zero away from the it, which is expected due to large stiffness of the rock. This example demonstrates the ability of the proposed method to handle irregularly shaped domains with a computationally challenging set of parameters, which are realistic for hydraulic fracturing in tight rock formations.

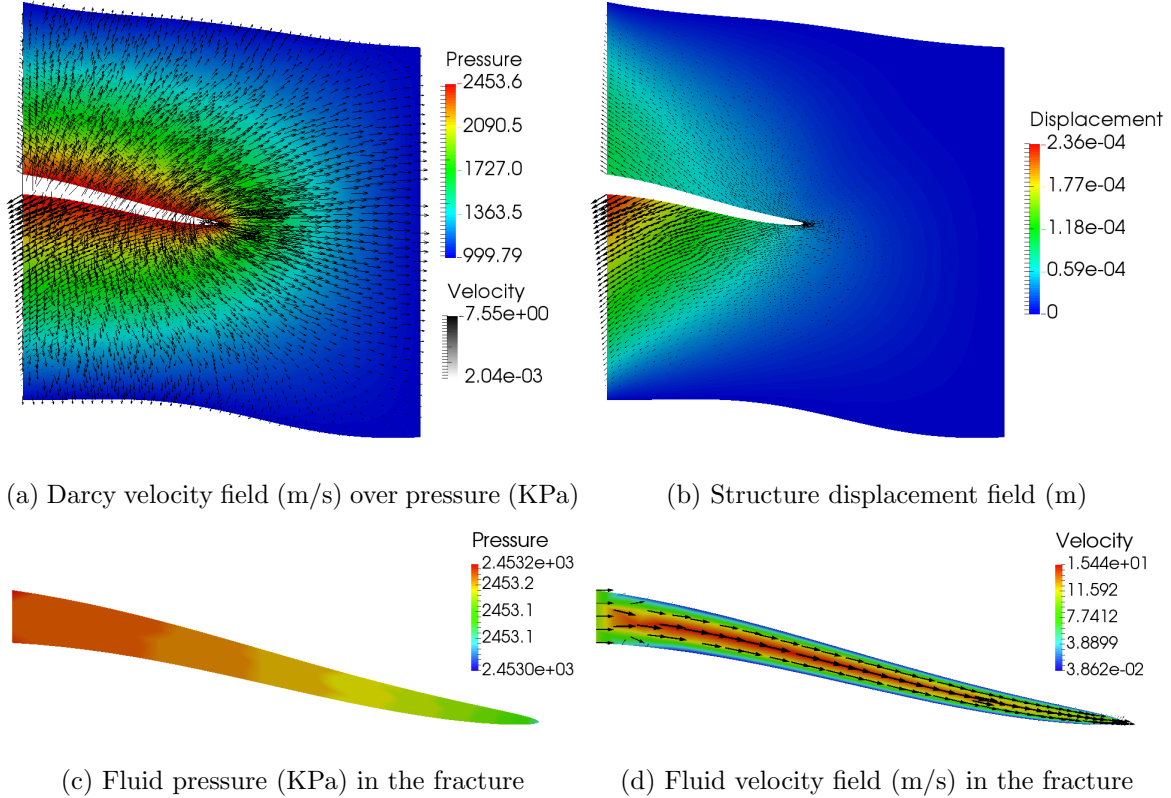


Figure 2: Example 2: fluid flow in a fractured reservoir,  $t = 300$  s.

### 7.3 Flow through fractured reservoir with heterogeneous permeability

In this example we illustrate the ability of the method to handle heterogeneous permeability and Young's modulus. For this simulation we use the reference domain  $\hat{\Omega}$ , see Figure 1b. The same boundary and initial conditions as in the previous test case are specified, and the same physical parameters from Table 3 are used, except for the permeability  $K$  and the Young's modulus  $E$ . The permeability and porosity data is taken from a two-dimensional cross-section of the data provided by the Society of Petroleum Engineers (SPE) Comparative Solution Project<sup>1</sup>. The SPE data, which is given on a rectangular  $60 \times 220$  grid is projected onto the triangular grid on the reference domain  $\hat{\Omega}$ , and visualized in Figure 3. We note that the permeability tensor is isotropic in this example. Given the porosity  $\phi$  the Young's modulus is determined from the law

$$E = 10^7 \left(1 - \frac{\phi}{c}\right)^{2.1},$$

where the constant  $c = 0.5$  refers to the porosity at which the effective Young's modulus becomes zero. This constant is chosen in general based on the properties of the porous medium. The justification for this law can be found in [31].

The simulation results at the final time  $T = 300$ s are shown in Figure 4. Figures 4a and 4b show that the propagation of the fluid in the Darcy region, as evidenced by the variation in the velocity and pressure, follows the contours of regions of higher permeability seen in Figure 3b). As in the previous test case, the highest velocity in the reservoir is near the fracture tip. However, the leak-off

<sup>1</sup>[www.spe.org/web/csp](http://www.spe.org/web/csp)



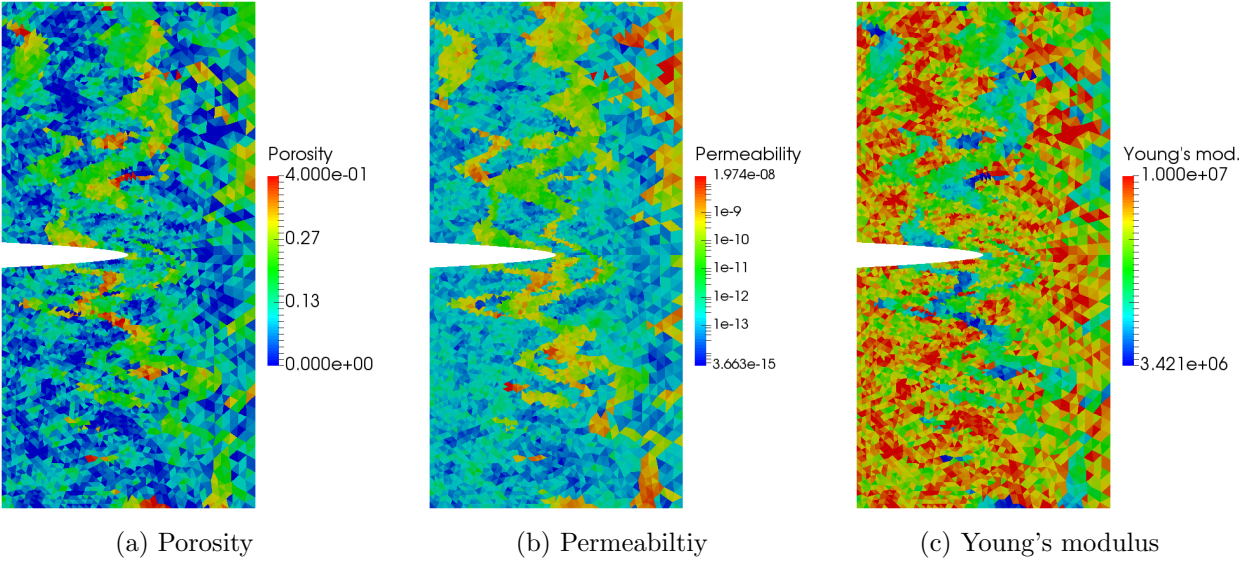


Figure 3: Heterogeneous material coefficients in Example 3.

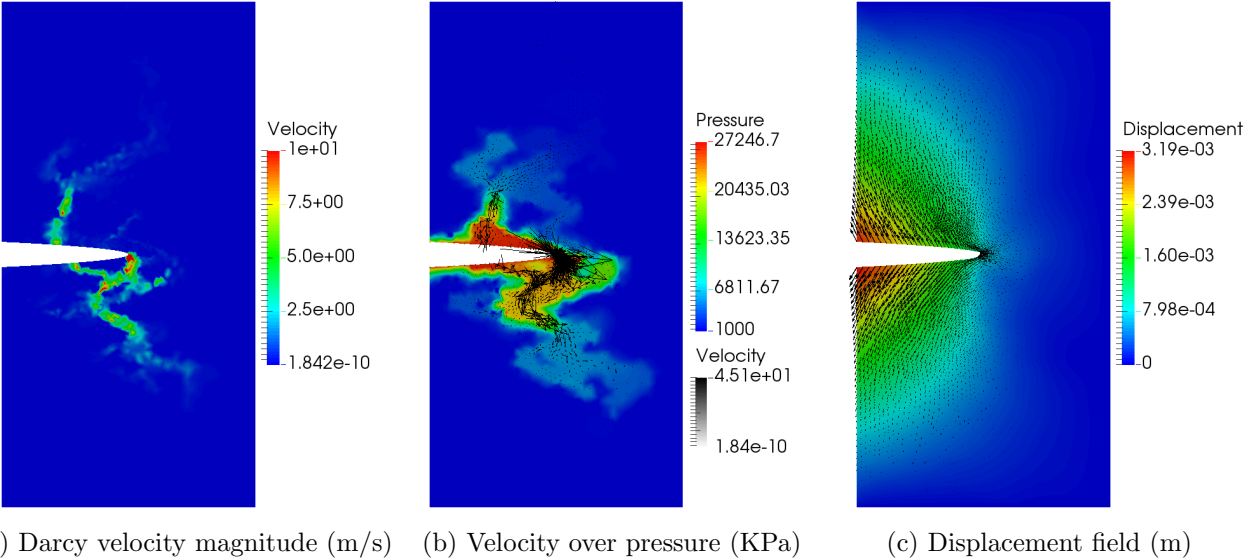


Figure 4: Example 3: fluid flow in a fractured reservoir with heterogeneous permeability and Young's modulus,  $t = 300$  s.

along the fracture is less uniform, with a significant leak-off near the middle-top of the fracture due to the region of relatively high permeability located there. The last Figure 4c depicts the nonuniform displacement field in the reservoir caused by the heterogeneous Young's modulus. We note that the effect of heterogeneity of the elastic coefficients is less pronounced due to the large stiffness of the rock. The general displacement profile is similar to the homogeneous case.

## 7.4 Sensitivity analysis

The goal of this section is to investigate how the developed model behaves when the parameters are modified, moving from mild non-physical values toward more realistic values that resemble the ones used in the hydraulic fracturing examples. We progressively update the parameters  $K$ ,  $s_0$  and  $E$  as shown in Table 4, while the rest of the parameters are taken from Table 3. All test cases in this section are governed by the same boundary and initial conditions as in the previous two examples.

|   | $K$ (m <sup>2</sup> )                  | $s_0$ (KPa <sup>-1</sup> ) | $E$ (KPa) |
|---|--|----------------------------|-----------|
| A | $\mathbf{I} \times 10^{-6}$            | 1.0                        | $10^3$    |
| B | $\text{diag}(200, 50) \times 10^{-12}$ | 1.0                        | $10^3$    |
| C | $\text{diag}(200, 50) \times 10^{-12}$ | $10^{-2}$                  | $10^3$    |
| D | $\text{diag}(200, 50) \times 10^{-12}$ | $10^{-2}$                  | $10^{10}$ |

Table 4: Set of parameters for the sensitivity analysis in Example 4.

**Case A:** The pressure gradient is small as seen from the contour plot, this is due to the large permeability. Also, from continuity of flux across the interface, one would expect to see that the magnitude of the Darcy velocity is close to the magnitude of the Stokes velocity, which we indeed observe in all the simulations.

**Case B:** The permeability now is 4 orders of magnitude smaller, resulting in a larger pressure gradient, which is consistent with Darcy’s law (2.4). Also, more flow is going toward the tip of the fracture, since its walls are now much less permeable. The displacement magnitude is also larger, while keeping the same profile.

**Case C:** This case shows how the model reacts to decrease in mass storativity - which is by exhibiting larger pressure gradient and displacement magnitude while keeping the overall behavior as in case B.

**Case D:** The last case is to show the effect of a significant change in Young’s modulus. Increasing it by 7 orders of magnitude, which makes the material much stiffer, results in the displacement being decreased by 7 orders of magnitude as expected.

The above results show that the displacement magnitude directly increases with the magnitude of the pressure, while the profile of the displacement field stays the same. This is consistent with the dependence of the poroelastic stress on the fluid pressure, see (2.3). In addition, the displacement magnitude is inversely proportional to the Young’s modulus, which is consistent with the constitutive law for the elastic stress in (2.3).

## 8 Conclusions

We have studied the interaction of a free fluid with a fluid within a poroelastic medium. After stating the governing equations and discussing the appropriate boundary and interface conditions we considered a numerical discretization of the problem using a mixed finite element method. A Lagrange multiplier is used to impose weakly the continuity of normal velocity interface condition, which is of essential type

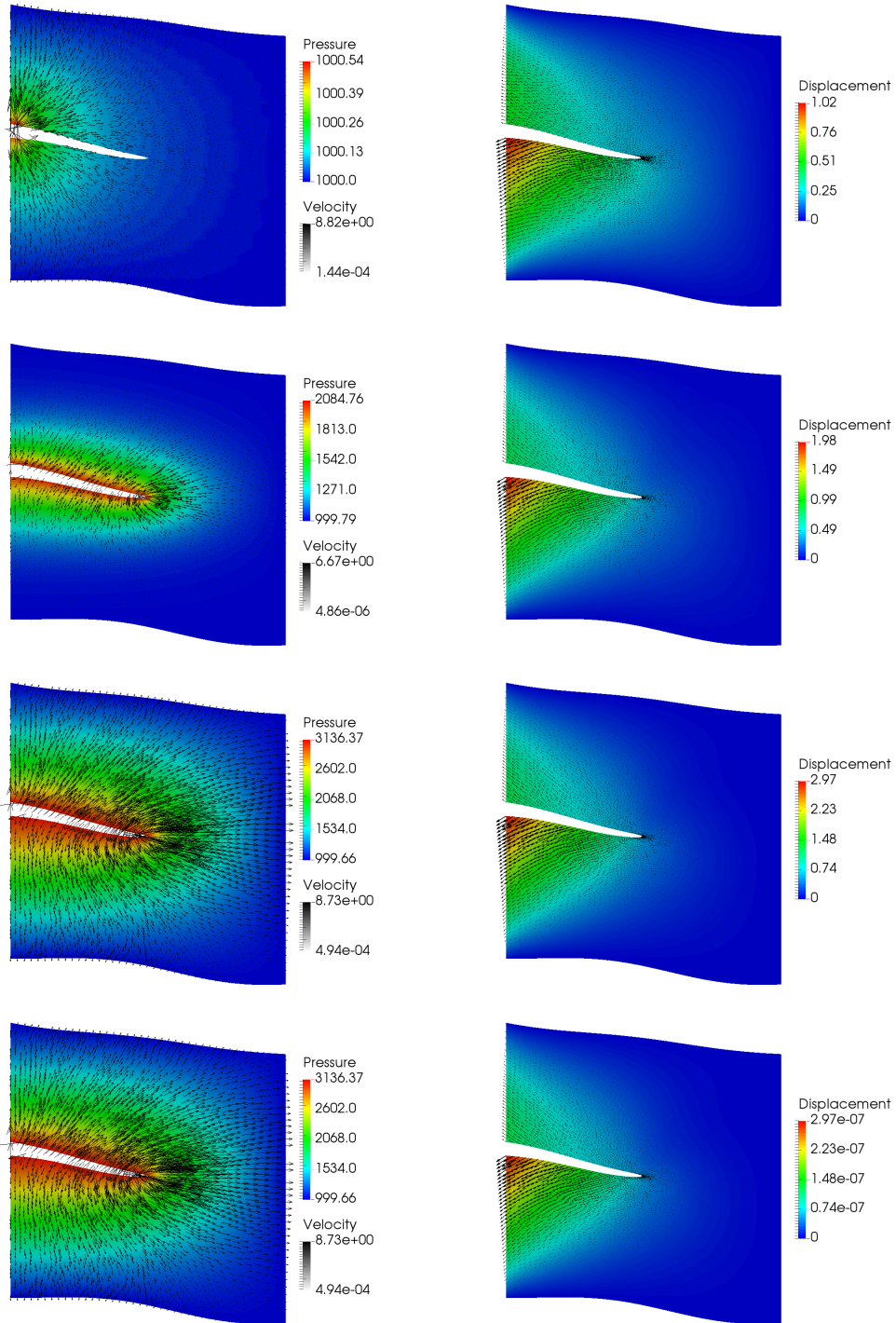


Figure 5: Sensitivity analysis simulations,  $t = 300$  s. Cases A to D are shown from top to bottom. The left figures show the Darcy velocity (m/s) superimposed with contour plot for the pressure (KPa). The right figures show the structure displacement field (m) over the displacement magnitude contour plot. The grayscale velocity legend shows the range of velocity magnitude.

in the mixed Darcy formulation. We show that the method is stable and convergent of optimal order, even in the case of non-matching grids across the interface. Computational experiments illustrate that this method is an effective approach for simulating fluid-poroelastic structure interaction with a wide range of physical parameters, including heterogeneous media. The Lagrange multiplier formulation is suitable for parallel non-overlapping domain decomposition algorithms and multiscale approximations via coarse mortar spaces. These topics will be explored in future research.

## 9 Appendix: fully discrete analysis

In this section we provide a detailed analysis of the stability and convergence of the fully discrete method (6.1)-(6.3). We will utilize the following discrete Gronwall inequality [43].

**Lemma 9.1** (Discrete Gronwall lemma). *Let  $\tau > 0$ ,  $B \geq 0$ , and let  $a_n, b_n, c_n, d_n$ ,  $n \geq 0$ , be non-negative sequences such that  $a_0 \leq B$  and*

$$a_n + \tau \sum_{l=1}^n b_l \leq \tau \sum_{l=1}^{n-1} d_l a_l + \tau \sum_{l=1}^n c_l + B, \quad n \geq 1.$$

Then,

$$a_n + \tau \sum_{l=1}^n b_l \leq \exp\left(\tau \sum_{l=1}^{n-1} d_l\right) \left( \tau \sum_{l=1}^n c_l + B \right), \quad n \geq 1.$$

*Proof of Theorem 6.1.* We choose

$$(\mathbf{v}_{f,h}, w_{f,h}, \mathbf{v}_{p,h}, w_{p,h}, \boldsymbol{\xi}_{p,h}, \mu_h) = (\mathbf{u}_{f,h}^n, p_{f,h}^n, \mathbf{u}_{p,h}^n, p_{p,h}^n, d_\tau \boldsymbol{\eta}_{p,h}^n, \lambda_h)$$

in (6.1)–(6.3) and use the discrete analog of (3.17):

$$\int_S u^n d_\tau \phi^n = \frac{1}{2} d_\tau \|\phi^n\|_{L^2(S)}^2 + \frac{1}{2} \tau \|d_\tau \phi^n\|_{L^2(S)}^2 \quad (9.1)$$

to obtain the energy equality

$$\begin{aligned} & \frac{1}{2} d_\tau \left( s_0 \|p_{p,h}^n\|_{L^2(\Omega_p)}^2 + a_p^\varepsilon(\boldsymbol{\eta}_{p,h}^n, \boldsymbol{\eta}_{p,h}^n) \right) + \frac{\tau}{2} \left( s_0 \|d_\tau p_{p,h}^n\|_{L^2(\Omega_p)}^2 + a_p^\varepsilon(d_\tau \boldsymbol{\eta}_{p,h}^n, d_\tau \boldsymbol{\eta}_{p,h}^n) \right) \\ & + a_f(\mathbf{u}_{f,h}^n, \mathbf{u}_{f,h}^n) + a_p^d(\mathbf{u}_{p,h}^n, \mathbf{u}_{p,h}^n) + |\mathbf{u}_{f,h}^n - d_\tau \boldsymbol{\eta}_{p,h}^n|_{a_{BJS}}^2 = \mathcal{F}(t_n). \end{aligned} \quad (9.2)$$

The right-hand side can be bounded as follows, using inequalities (4.1) and (4.3),

$$\begin{aligned} \mathcal{F}(t_n) &= (\mathbf{f}_f(t_n), \mathbf{u}_{f,h}^n) + (\mathbf{f}_p(t_n), d_\tau \boldsymbol{\eta}_{p,h}^n) + (q_f(t_n), p_{f,h}^n) + (q_p(t_n), p_{p,h}^n) \\ &\leq (\mathbf{f}_p(t_n), d_\tau \boldsymbol{\eta}_{p,h}^n) + \frac{\epsilon_1}{2} \left( \|\mathbf{u}_{f,h}^n\|_{L^2(\Omega_f)}^2 + \|p_{f,h}^n\|_{L^2(\Omega_f)}^2 + \|p_{p,h}^n\|_{L^2(\Omega_p)}^2 \right) \\ &\quad + C \frac{1}{2\epsilon_1} \left( \|\mathbf{f}_f(t_n)\|_{L^2(\Omega_f)}^2 + \|q_f(t_n)\|_{L^2(\Omega_f)}^2 + \|q_p(t_n)\|_{L^2(\Omega_p)}^2 \right). \end{aligned} \quad (9.3)$$

Combining (9.2) and (9.3), summing up over the time index  $n = 1, \dots, N$ , multiplying by  $\tau$  and using the coercivity of the bilinear forms (3.4)–(3.6), we obtain

$$\begin{aligned}
& s_0 \|p_{p,h}^N\|_{L^2(\Omega_p)}^2 + \|\boldsymbol{\eta}_{p,h}^N\|_{H^1(\Omega_p)}^2 + \tau \sum_{n=1}^N \left( \|\mathbf{u}_{f,h}^n\|_{H^1(\Omega_f)}^2 + \|\mathbf{u}_{p,h}^n\|_{L^2(\Omega_p)}^2 + |\mathbf{u}_{f,h}^n - d_\tau \boldsymbol{\eta}_{p,h}^n|_{a_{BJS}}^2 \right) \\
& + \tau^2 \sum_{n=1}^N \left( s_0 \|d_\tau p_{p,h}^n\|_{L^2(\Omega_p)}^2 + \|d_\tau \boldsymbol{\eta}_{p,h}^n\|_{H^1(\Omega_p)}^2 \right) \\
& \leq C \left( s_0 \|p_{p,h}^0\|_{L^2(\Omega_p)}^2 + \|\boldsymbol{\eta}_{p,h}^0\|_{H^1(\Omega_p)}^2 + \epsilon_1 \tau \sum_{n=1}^N \left( \|\mathbf{u}_{f,h}^n\|_{L^2(\Omega_f)}^2 + \|p_{f,h}^n\|_{L^2(\Omega_f)}^2 + \|p_{p,h}^n\|_{L^2(\Omega_p)}^2 \right) \right. \\
& \left. + \epsilon_1^{-1} \tau \sum_{n=1}^N \left( \|\mathbf{f}_f(t_n)\|_{L^2(\Omega_f)}^2 + \|q_f(t_n)\|_{L^2(\Omega_f)}^2 + \|q_p(t_n)\|_{L^2(\Omega_p)}^2 \right) + \tau \sum_{n=1}^N (\mathbf{f}_p(t_n), d_\tau \boldsymbol{\eta}_{p,h}^n) \right). \quad (9.4)
\end{aligned}$$

To bound the last term on the right we use summation by parts:

$$\begin{aligned}
\tau \sum_{n=1}^N (\mathbf{f}_p(t_n), d_\tau \boldsymbol{\eta}_{p,h}^n) &= (\mathbf{f}_p(t_N), \boldsymbol{\eta}_{p,h}^N) - (\mathbf{f}_p(0), \boldsymbol{\eta}_{p,h}^0) - \tau \sum_{n=1}^{N-1} (d_\tau \mathbf{f}_p^n, \boldsymbol{\eta}_{p,h}^n) \\
&\leq \frac{\epsilon_1}{2} \|\boldsymbol{\eta}_{p,h}^N\|_{L^2(\Omega_p)}^2 + \frac{1}{2\epsilon_1} \|\mathbf{f}_p(t_N)\|_{L^2(\Omega_p)}^2 + \frac{\tau}{2} \sum_{n=1}^{N-1} \|\boldsymbol{\eta}_{p,h}^n\|_{L^2(\Omega_p)}^2 \\
&\quad + \frac{1}{2} \left( \|\boldsymbol{\eta}_{p,h}^0\|_{L^2(\Omega_p)}^2 + \|\mathbf{f}_p(0)\|_{L^2(\Omega_p)}^2 + \tau \sum_{n=1}^{N-1} \|d_\tau \mathbf{f}_p^n\|_{L^2(\Omega_p)}^2 \right). \quad (9.5)
\end{aligned}$$

Next using the inf-sup condition (3.9) for  $(p_{f,h}^n, p_{p,h}^n, \lambda_h^n)$  we obtain, in a similar way to (4.8),

$$\begin{aligned}
& \epsilon_2 \tau \sum_{n=1}^N \left( \|p_{f,h}^n\|_{L^2(\Omega_f)}^2 + \|p_{p,h}^n\|_{L^2(\Omega_p)}^2 + \|\lambda_h^n\|_{\Lambda_h}^2 \right) \\
& \leq C \epsilon_2 \tau \sum_{n=1}^N \left( \|\mathbf{f}_f(t_n)\|_{L^2(\Omega_f)}^2 + \|\mathbf{f}_p(t_n)\|_{L^2(\Omega_p)}^2 + \|\mathbf{u}_{f,h}^n\|_{H^1(\Omega_f)}^2 + \|\mathbf{u}_{p,h}^n\|_{L^2(\Omega_p)}^2 \right. \\
& \quad \left. + \|\boldsymbol{\eta}_{p,h}^n\|_{H^1(\Omega_p)}^2 + |\mathbf{u}_{f,h}^n - d_\tau \boldsymbol{\eta}_{p,h}^n|_{a_{BJS}}^2 \right). \quad (9.6)
\end{aligned}$$

Combining (9.4)–(9.6), and taking  $\epsilon_2$  small enough, and then  $\epsilon_1$  small enough, and using Lemma 9.1 with  $a_n = \|\boldsymbol{\eta}_{p,h}^n\|_{H^1(\Omega_p)}^2$ , gives

$$\begin{aligned}
& s_0 \|p_{p,h}^N\|_{L^2(\Omega_p)}^2 + \|\boldsymbol{\eta}_{p,h}^N\|_{H^1(\Omega_p)}^2 + \tau \sum_{n=1}^N \left[ \|\mathbf{u}_{f,h}^n\|_{H^1(\Omega_f)}^2 + \|\mathbf{u}_{p,h}^n\|_{L^2(\Omega_p)}^2 + |\mathbf{u}_{f,h}^n - d_\tau \boldsymbol{\eta}_{p,h}^n|_{a_{BJS}}^2 \right] \\
& + \tau^2 \sum_{n=1}^N \left[ s_0 \|d_\tau p_{p,h}^n\|_{L^2(\Omega_p)}^2 + \|d_\tau \boldsymbol{\eta}_{p,h}^n\|_{H^1(\Omega_p)}^2 \right] + \tau \sum_{n=1}^N \left[ \|p_{p,h}^n\|_{L^2(\Omega_p)}^2 + \|p_{f,h}^n\|_{L^2(\Omega_f)}^2 + \|\lambda_h^n\|_{\Lambda_h}^2 \right] \\
& \leq C \exp(T) \left( s_0 \|p_{p,h}^0\|_{L^2(\Omega_p)}^2 + \|\boldsymbol{\eta}_{p,h}^0\|_{H^1(\Omega_p)}^2 + \|\mathbf{f}_p(0)\|_{L^2(\Omega_p)}^2 \right. \\
& \quad \left. + \tau \sum_{n=1}^N \left[ \|\mathbf{f}_f(t_n)\|_{L^2(\Omega_f)}^2 + \|\mathbf{f}_p(t_n)\|_{L^2(\Omega_p)}^2 + \|q_f(t_n)\|_{L^2(\Omega_f)}^2 + \|q_p(t_n)\|_{L^2(\Omega_p)}^2 + \|d_\tau \mathbf{f}_p\|_{L^2(\Omega_p)}^2 \right] \right),
\end{aligned}$$

which implies the statement of the theorem using the appropriate space-time norms.  $\square$

For the sake of space, we do not present the proof of Theorem 6.2. The error equations are obtained by subtracting the first two equations of the fully discrete formulation (6.1)–(6.2) from their continuous counterparts (2.10)–(2.11):

$$\begin{aligned}
& a_f(\mathbf{e}_f^n, \mathbf{v}_{f,h}) + a_p^d(\mathbf{e}_p^n, \mathbf{v}_{p,h}) + a_p^e(\mathbf{e}_s^n, \boldsymbol{\xi}_{p,h}) + a_{BJS}(\mathbf{e}_f^n, d_\tau \mathbf{e}_s^n; \mathbf{v}_{f,h}, \boldsymbol{\xi}_{p,h}) + b_f(\mathbf{v}_{f,h}, e_{fp}^n) + b_p(\mathbf{v}_{p,h}, e_{pp}^n) \\
& + \alpha b_p(\boldsymbol{\xi}_{p,h}, e_{pp}^n) + b_\Gamma(\mathbf{v}_{f,h}, \mathbf{v}_{p,h}, \boldsymbol{\xi}_{p,h}; e_\lambda^n) + (s_0 d_\tau e_{pp}^n, w_{p,h}) - \alpha b_p(d_\tau e_s^n, w_{p,h}) - b_p(\mathbf{e}_p^n, w_{p,h}) \\
& - b_f(\mathbf{e}_f^n, w_{f,h}) = (s_0 r_n(p_p), w_{p,h}) + a_{BJS}(0, r_n(\boldsymbol{\eta}_p); \mathbf{v}_{f,h}, \boldsymbol{\xi}_{p,h}) - \alpha b_p(r_n(\boldsymbol{\eta}_p), w_{p,h}), \tag{9.7}
\end{aligned}$$

where  $r_n$  denotes the difference between the time derivative and its discrete analog:

$$r_n(\theta) = \partial_t \theta(t_n) - d_\tau \theta^n.$$

It is easy to see that [10, Lemma 4] for sufficiently smooth  $\theta$ ,

$$\tau \sum_{n=1}^N \|r_n(\theta)\|_{H^k(S)}^2 \leq C\tau^2 \|\partial_{tt}\theta\|_{L^2(0,T;H^k(S))}^2.$$

The proof of Theorem 6.2 follows the structure of the proof of Theorem 5.1, using discrete-in-time arguments as in the proof of Theorem 6.1.

## References

- [1] I. Ambartsumyan, E. Khattatov, I. Yotov, and P. Zunino. Simulation of flow in fractured poroelastic media: a comparison of different discretization approaches. In *Finite difference methods, theory and applications*, volume 9045 of *Lecture Notes in Comput. Sci.*, pages 3–14. Springer, Cham, 2015.
- [2] T. Arbogast, G. Pencheva, M. F. Wheeler, and I. Yotov. A multiscale mortar mixed finite element method. *Multiscale Model. Simul.*, 6(1):319–346, 2007.
- [3] D. N. Arnold, F. Brezzi, and M. Fortin. A stable finite element for the Stokes equations. *Calcolo*, 21(4):337–344, 1984.
- [4] S. Badia, A. Quaini, and A. Quarteroni. Coupling Biot and Navier-Stokes equations for modelling fluid-poroelastic media interaction. *J. Comput. Phys.*, 228(21):7986–8014, 2009.
- [5] G. S. Beavers and D. D. Joseph. Boundary conditions at a naturally impermeable wall. *J. Fluid. Mech.*, 30:197–207, 1967.
- [6] M. Biot. General theory of three-dimensional consolidation. *J. Appl. Phys.*, 12:155–164, 1941.
- [7] D. Boffi, F. Brezzi, and M. Fortin. *Mixed finite element methods and applications*, volume 44 of *Springer Series in Computational Mathematics*. Springer, Heidelberg, 2013.
- [8] K. Brenan, S. Campbell, and L. Petzold. *Numerical Solution of Initial-Value Problems in Differential-Algebraic Equations*. 1995.
- [9] M. Bukac, I. Yotov, R. Zakerzadeh, and P. Zunino. Partitioning strategies for the interaction of a fluid with a poroelastic material based on a Nitsche’s coupling approach. *Comput. Methods Appl. Mech. Engrg.*, 292:138–170, 2015.

- [10] M. Bukac, I. Yotov, and P. Zunino. An operator splitting approach for the interaction between a fluid and a multilayered poroelastic structure. *Numer. Methods Partial Differential Equations*, 31(4):1054–1100, 2015.
- [11] M. Bukac, I. Yotov, and P. Zunino. Dimensional model reduction for flow through fractures in poroelastic media. *ESAIM Math. Model. Numer. Anal.*, <http://dx.doi.org/10.1051/m2an/2016069>, 2016.
- [12] E. Burman and M. A. Fernández. Stabilization of explicit coupling in fluid-structure interaction involving fluid incompressibility. *Comput. Methods Appl. Mech. Engrg.*, 198(5-8):766–784, 2009.
- [13] E. Burman and M. A. Fernández. Explicit strategies for incompressible fluid-structure interaction problems: Nitsche type mortaring versus Robin-Robin coupling. *Internat. J. Numer. Methods Engrg.*, 97(10):739–758, 2014.
- [14] P. Ciarlet. *The finite element method for elliptic problems*, volume 4. North Holland, 1978.
- [15] C. D’Angelo and A. Scotti. A mixed finite element method for Darcy flow in fractured porous media with non-matching grids. *ESAIM: Math. Model. Numer. Anal.*, 46(2):465–489, 2012.
- [16] S. Deparis, M. Discacciati, G. Fourestey, and A. Quarteroni. Fluid-structure algorithms based on Steklov-Poincaré operators. *Comput. Methods Appl. Mech. Engrg.*, 195(41-43):5797–5812, 2006.
- [17] M. Discacciati, E. Miglio, and A. Quarteroni. Mathematical and numerical models for coupling surface and groundwater flows. *Appl. Numer. Math.*, 43(1-2):57–74, 2002.
- [18] A. Ern and J.-L. Guermond. *Theory and practice of finite elements*, volume 159 of *Applied Mathematical Sciences*. Springer-Verlag, New York, 2004.
- [19] M. A. Fernández. Incremental displacement-correction schemes for the explicit coupling of a thin structure with an incompressible fluid. *Comptes Rendus Mathématique*, 349(7):473–477, 2011.
- [20] N. Frih, V. Martin, J. E. Roberts, and A. Saada. Modeling fractures as interfaces with nonmatching grids. *Comput. Geosci.*, 16(4):1043–1060, 2012.
- [21] N. Frih, J. E. Roberts, and A. Saada. Modeling fractures as interfaces: a model for Forchheimer fractures. *Comput. Geosci.*, 12(1):91–104, 2008.
- [22] A. Fumagalli and A. Scotti. Numerical modelling of multiphase subsurface flow in the presence of fractures. *Commun. Appl. Ind. Math.*, 3(1):e–380, 23, 2012.
- [23] J. Galvis and M. Sarkis. Non-matching mortar discretization analysis for the coupled Stokes-Darcy equations. *Electronic Transactions on Numerical Analysis*, 26:350–384, 2007.
- [24] B. Ganis, M. E. Mear, A. Sakhaee-Pour, M. F. Wheeler, and T. Wick. Modeling fluid injection in fractures with a reservoir simulator coupled to a boundary element method. *Comput. Geosci.*, 18(5):613–624, 2014.
- [25] B. Ganis and I. Yotov. Implementation of a mortar mixed finite element method using a multiscale flux basis. *Comput. Methods Appl. Mech. Engrg.*, 198(49-52):3989–3998, 2009.
- [26] V. Girault and B. Rivière. DG approximation of coupled Navier-Stokes and Darcy equations by Beaver-Joseph-Saffman interface condition. *SIAM J. Numer. Anal.*, 47(3):2052–2089, 2009.

- [27] V. Girault, D. Vassilev, and I. Yotov. Mortar multiscale finite element methods for Stokes-Darcy flows. *Numer. Math.*, 127(1):93–165, 2014.
- [28] V. Girault, M. F. Wheeler, B. Ganis, and M. E. Mear. A lubrication fracture model in a poro-elastic medium. *Math. Models Methods Appl. Sci.*, 25(4):587–645, 2015.
- [29] P. Grisvard. *Elliptic problems in nonsmooth domains*. Pitman, Boston, 1985.
- [30] F. Hecht. New development in FreeFem++. *J. Numer. Math.*, 20(3-4):251–265, 2012.
- [31] J. Kovacic. Correlation between Young’s modulus and porosity in porous materials. *Journal of materials science letters*, 18(13):1007–1010, 1999.
- [32] W. J. Layton, F. Schieweck, and I. Yotov. Coupling fluid flow with porous media flow. *SIAM J. Numer. Anal.*, 40(6):2195–2218, 2003.
- [33] S. Lee, M. F. Wheeler, and T. Wick. Pressure and fluid-driven fracture propagation in porous media using an adaptive finite element phase field model. *Comput. Methods Appl. Mech. Engrg.*, 305:111–132, 2016.
- [34] M. Lesinigo, C. D’Angelo, and A. Quarteroni. A multiscale Darcy–Brinkman model for fluid flow in fractured porous media. *Numer. Math.*, 117(4):717–752, 2011.
- [35] J. L. Lions and E. Magenes. *Non-homogeneous boundary value problems and applications*, volume 1. Springer-Verlag, 1972.
- [36] V. Martin, J. Jaffre, and J. E. Roberts. Modeling fractures and barriers as interfaces for flow in porous media. *SIAM J. Sci. Comput.*, 26(5):1667–1691, 2005.
- [37] T. P. Mathew. *Domain decomposition and iterative refinement methods for mixed finite element discretizations of elliptic problems*. PhD thesis, Courant Institute of Mathematical Sciences, New York University, 1989. Tech. Rep. 463.
- [38] A. Mikelić, M. F. Wheeler, and T. Wick. Phase-field modeling of a fluid-driven fracture in a poroelastic medium. *Comput. Geosci.*, 19(6):1171–1195, 2015.
- [39] F. Morales and R. E. Showalter. The narrow fracture approximation by channeled flow. *J. Math. Anal. Appl.*, 365(1):320–331, 2010.
- [40] M. Mu and J. Xu. A two-grid method of a mixed Stokes-Darcy model for coupling fluid flow with porous media flow. *SIAM J. Numer. Anal.*, 45(5):1801–1813, 2007.
- [41] F. Nobile and C. Vergara. An effective fluid-structure interaction formulation for vascular dynamics by generalized Robin conditions. *SIAM J. Sci. Comput.*, 30:731–763, 2008.
- [42] A. Quaini and A. Quarteroni. A semi-implicit approach for fluid-structure interaction based on an algebraic fractional step method. *Math. Models Methods Appl. Sci.*, 17(6):957–985, 2007.
- [43] A. Quarteroni and A. Valli. *Numerical approximation of partial differential equations*, volume 23 of *Springer Series in Computational Mathematics*. Springer-Verlag, Berlin, 1994.
- [44] P.-A. Raviart and J.-M. Thomas. A mixed finite element method for 2-nd order elliptic problems. In *Mathematical aspects of finite element methods*, pages 292–315. Springer, 1977.



- [45] B. Rivière and I. Yotov. Locally conservative coupling of Stokes and Darcy flows. *SIAM J. Numer. Anal.*, 42(5):1959–1977, 2005.
- [46] P. G. Saffman. On the boundary condition at the surface of a porous media. *Stud. Appl. Math., L*, (2):93–101, 1971.
- [47] L. R. Scott and S. Zhang. Finite element interpolation of nonsmooth functions satisfying boundary conditions. *Math. Comp.*, 54(190):483–493, 1990.
- [48] R. E. Showalter. Poroelastic filtration coupled to Stokes flow. In *Control theory of partial differential equations*, volume 242 of *Lect. Notes Pure Appl. Math.*, pages 229–241. Chapman & Hall/CRC, Boca Raton, FL, 2005.
- [49] R. E. Showalter. Nonlinear degenerate evolution equations in mixed formulation. *SIAM J. Math. Anal.*, 42(5):2114–2131, 2010.
- [50] C. Taylor and P. Hood. A numerical solution of the Navier-Stokes equations using the finite element technique. *Computers & Fluids*, 1(1):73–100, 1973.
- [51] D. Vassilev, C. Wang, and I. Yotov. Domain decomposition for coupled Stokes and Darcy flows. *Comput. Methods Appl. Mech. Engrg.*, 268:264–283, 2014.
- [52] X. Xie, J. Xu, and G. Xue. Uniformly-stable finite element methods for Darcy-Stokes-Brinkman models. *J. Comput. Math.*, 26(3):437–455, 2008.
- [53] J. Xu and K. Yang. Well-posedness and robust preconditioners for discretized fluid-structure interaction systems. *Comput. Methods Appl. Mech. Engrg.*, 292:69–91, 2015.
- [54] S.-Y. Yi. Convergence analysis of a new mixed finite element method for Biot’s consolidation model. *Numer. Methods Partial Differential Eq.*, 30(4):1189–1210, 2014.